R. & M. No. 3645

R. & M. No. 3645

MINISTRY OF TECHNOLOGY

AERONAUTICAL RESEARCH COUNCIL
REPORTS AND MEMORANDA

The Behaviour of the Leading-Edge Vortices over a Delta Wing Following a Sudden Change of Incidence

By N. C. LAMBOURNE, D. W. BRYER and J. F. M. MAYBREY
Aerodynamics Division N.P.L.

LONDON: HER MAJESTY'S STATIONERY OFFICE
1970
PRICE £1 5*s* 0*d* [£1·25] NET

The Behaviour of the Leading-Edge Vortices over a Delta Wing Following a Sudden Change of Incidence

By N. C. LAMBOURNE, D. W. BRYER and J. F. M. MAYBREY

Aerodynamics Division N.P.L.

Reports and Memoranda No. 3645*
March, 1969

Summary.

The transient behaviour of leading-edge vortices over a delta wing subject to a sudden change of incidence is of importance in understanding the wing loadings that can occur in unsteady conditions of flight. In the experiments reported here, changes of incidence have been imposed on delta-shaped plates by application of a constant-velocity plunging motion for a limited time; other related unsteady motions are discussed in the Appendix.

Ciné records of particle tracks and of dye filaments in a water tunnel have been analysed to trace the time history of vortex centres in cross-flow planes following the application of step-changes of incidence. The flows for various combinations of initial incidence, planform, plunging velocity and chordwise position have been examined.

Results indicate that after the start of the plunge an effectively steady vortex system is established over the plate in a time approximately equal to that required for one chord length of relative forward travel. Where comparisons can be made, Dore's theoretical calculations of the manner in which the vortices move show fair agreement with the experiment.

Effects of the transient movements of the vortices on lift distribution are discussed and the inference is drawn that the changes in the distribution of wing loading occurring for an increase of incidence are not simply reversed when the incidence is decreased.

CONTENTS

* Replaces NPL Aero Report 1294—A.R.C. 31 056

---

1. *Introduction.*

Over a wide range of angles of incidence, the flow over a slender delta wing involves two concentrated vortices that are generated by flow separation at the leading edges and which to a large extent determine the pressure distribution over the upper surface of the wing. The work which forms the subject of this report was started when the general nature of the vortex flow and the associated pressure distribution under steady conditions were already well understood but questions remained concerning the behaviour of the flow and associated aerodynamic loading under unsteady conditions of oscillatory or transient motion. It was considered that information about the flow under unsteady conditions would assist in understanding the unsteady loads. Accordingly, visual observations in a water tunnel were made of the flow occurring during certain types of oscillatory and transient motions of model wings with sharp leading edges; the observations obtained for the particular motion of a step-change of incidence caused by plunging the wing form the subject of the present report.

A problem of practical interest involving a change of wing incidence is the transient aerodynamic loading that occurs when an aircraft flies into an isolated gust. However, the simulation of a gust is not easily achieved in a tunnel but requires a special facility such as the open air gust track at the Royal Aircraft Establishment (Refs. 1, 2). The closest approximation to the change of incidence resulting from a sharp-edged gust that can be obtained by the application of a transient motion to a model in a tunnel is the sudden plunge. This, unlike the gust, does not include the passage of a front across the wing. It is relevant here to draw attention to the Appendix, which considers the distinctions between several types

of step-change, each of which results in a change of wing lift. Without entering into details here, we note that the type of incidence change used in the experiments, if applied to a two-dimensional wing, would result in a time-wise change of lift described by the Wagner function, whilst changes due to a sharp-edged gust would be described by the Küssner function.

With regard to the effect of a gust on a slender delta wing, a question of fundamental interest is posed by the following consideration. Supposing a delta-winged aircraft flying with incidence low enough to avoid flow separation meets a sudden gust which increases the incidence sufficiently for separation to occur at the leading edges, the question then arises—how do the leading-edge vortices first develop? Much of the present investigation is concerned with how the vortices develop after incidence is suddenly increased from zero.

The present experiments were conducted with three delta-shaped plates using water as the working fluid for ease of flow visualization. The changes of incidence which were applied were deliberately chosen to be large in order to exaggerate the changes of flow whilst the use of extremely low speeds of flow entailed a general time scale for which it was possible to engineer incidence changes that could be regarded as 'instantaneous'. The resulting values of Reynolds number are far below those of practice: however, when the plates are sharp-edged, the general nature of the flow is not likely to be so different from that at higher Reynolds numbers as to invalidate the application of the conclusions of the results.

The observations and measurements refer only to the behaviour of the vortices and the separated sheets from the leading edges. It was originally intended to determine the variation in vortex strength by a photographic technique of measuring particle velocities, but this aspect was abandoned when it became apparent that the analysis of the records would absorb an unacceptable amount of effort. Also, a rather restricted attempt was made with apparatus already available to measure transient changes in the lift, but this did not show sufficient promise of success.

Results of preliminary measurements were reported in 1962 (Ref. 3) and these suggested that the local flow over a delta wing had, for practical purposes, reached a new steady condition in approximately the time taken for the stream to move one chord length. Subsequent to these preliminary experiments, Dore[4] developed a theoretical treatment which yielded results directly comparable with the measurements. In case the conclusion of the earlier experiments should be peculiar to the particular aspect ratio of the wing that was used, further observations have now been made with higher and lower values of aspect ratio. Also, the amplitude of the incidence change and the initial value of the incidence have been varied. The present report covers the whole of the investigation and thus supersedes the previous note (Ref. 3).

2. *Experimental Method.*

2.1. *Models and Apparatus.*

The experiments were carried out in a water tunnel having a cross-section 0·33m × 0·25m. Three delta-shaped plates with leading apex angles 20°, 40° and 60° were used, details of their principal dimensions and the reference axes being given in Fig. 1. Each plate had the same general form, the 'upper' surface being flat and the 'lower' surface bevelled to provide sharp leading and trailing edges. The tunnel speed throughout the experiments was 0·13m/s (5in/s) which gave Reynolds numbers based on the root chords of about 2×10^4. Also indicated in Fig. 1 is the extent of the plunge displacement in relation to the tunnel cross section.

The general arrangement of apparatus is shown in Fig. 2. The plates were supported in the tunnel by a drive rod which passed through a gland in the tunnel back-plate to the connection with the driving mechanism. The drive rod was fixed to the delta plate by a single pivot which could be locked to set the initial incidence (α_A). The mechanical forcing gear shown in Figs. 2 and 3, consisted of a rotating disc driven by a variable-speed D.C. motor through a 1000 to 1 reduction gear. A peg in the face of the disc could be triggered to protrude and strike a cam attached to a sliding plate which drove the model across the flow at a constant velocity W for a distance of about 80mm (40mm on either side of the centre of the tunnel). This translation could be measured on a displacement transducer which showed that the initial acceleration took place in less than 1 per cent of the total plunge time. A friction pad brought the driving mechanism rapidly to rest when the peg left the cam. By changing the direction of rotation of the disc

and reversing the cam, the direction of the plunging motion could be reversed giving a decrease in effective incidence.

The speed of the motor, and hence the value of the plunge velocity W, could be monitored continuously by measuring the frequency at which a beam of light was interrupted by a perforated disc on the motor shaft. The quoted values of plunge velocities were, however, obtained more accurately from analysis of the film records. The tunnel velocity U was obtained by timing particles in the water over a measured distance in the free stream.

To visualise the flow, a beam of light (10mm thick) from a high-intensity carbon-arc lamp was projected across the tunnel and adjusted so as to intercept the delta plate at any chosen chordwise station, thus illuminating a cross-flow plane (Fig. 4).

2.2. *Quantitative Measurements of Vortex Position.*

Measurements of vortex position were obtained from photographs of suspended polystyrene particles which were visible whilst they passed through the beam of light. These particles had a specific gravity of approximately 1·02, a mean diameter 200 microns, and their paths were considered to represent the motion of fluid elements. When photographed through an inclined mirror from a position effectively well downstream of the model, as indicated in Fig. 4, particles in the undisturbed stream appeared as dots, whereas velocity components in the cross-flow plane led to the appearance on the ciné film of tracks of length proportional to particle velocity and frame exposure time. One frame from a typical film record is shown in Fig. 5*. To obtain good resolution, the field of the camera included only one of the pair of edge vortices and usually extended approximately from the plane of symmetry of the wing to a short distance outboard of the leading edge. The area of the flow field that was photographed was then about 56mm × 89mm; with the stated thickness of light beam, approximately 100 particles appeared in each photograph.

After preliminary trials of films and light sources, Eastman Double X film and a carbon-arc lamp (16 KVA) operating at a colour temperature of 5,800°K were used; the film was processed in a caustic developer to give maximum contrast.

For most quantitative measurements, six plunges were filmed, four at 8 frames/sec. and two at 16 frames/sec for each condition investigated. To afford a check on framing speeds, a timing disc driven by a synchronous motor was filmed immediately before each run. The choice of framing speeds was a compromise dictated by the thickness of the beam of light, the minimum acceptable track length required to determine the position of the vortex centre on the film and the number of ciné frames obtainable during the period of the transient motion. The camera shutter was not synchronised with the start of the plunge so that for each run the sequence of ciné frames was randomly phased with reference to the plunging motion.

A fine wire with two fixed markers at a known distance apart and held in the tunnel above the upper surface provided a datum line to give a dimensional calibration of the photographs and to deduce the instantaneous positions of the wing.

Estimations of the position of the vortex centre were made visually during frame-by-frame analysis of the ciné records. The film assessor that was used was provided with traversing cross-wires which could be aligned with the vortex centre, whose co-ordinates, together with those of the frame and wing reference points, could then be transferred to punch tape. The data was later processed by computer to give the co-ordinates of the vortex centre relative to the moving wing for a series of times measured from the start of the plunge.

2.3. *Qualitative Investigations.*

In order to study the formation of the vortices from the vortex layers springing from the leading edge and to examine certain effects of the plunge both on the vortices and the vortex layers, a special dye-

---

*Some particles appear as interrupted tracks because the shutter was modified to give three exposures per frame with the original intention of measuring particle velocities.

injection model was used. It took the form of a 40° delta plate basically of the same dimensions as that already described except for its thickness, which was 1·5 times the original in order to accommodate an internal chamber from which dye could be released from a series of narrow slots in one leading edge; the extent of the slots was from about 0·35 to 0·58 of the length of the edge, measured from the apex. Controlled emission of dye during a plunge stained the fluid sheet from the leading edge. Ciné records were taken using the same camera position and lighting as used in the particle experiments; the full extent of the shear layer at any one station was not visible owing to the limited extent of the dye emission along the leading edge.

3. *Applied Incidence Changes.*

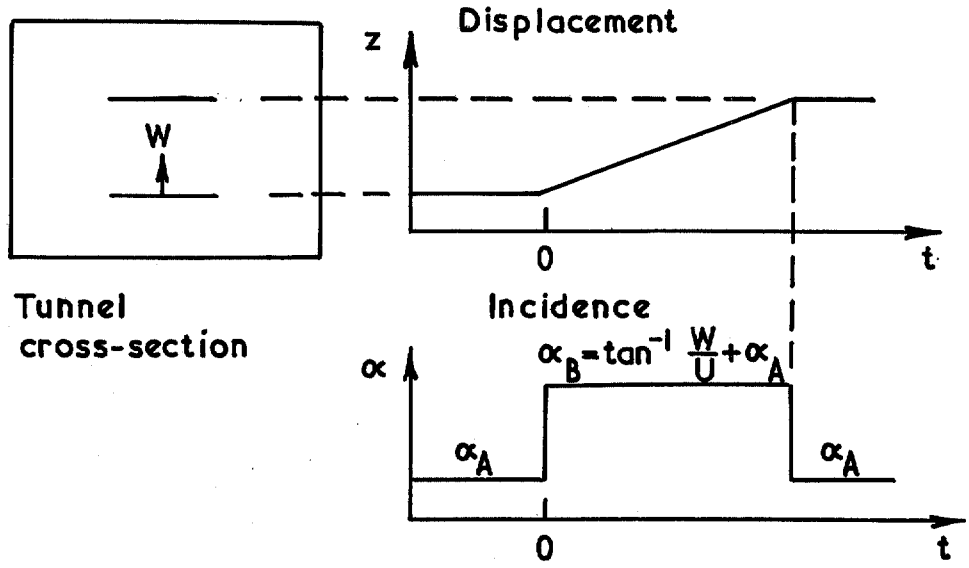

The changes of incidence applied to a wing are related to the plunging motion by the above diagram. At time $t = 0$, there is a sudden increase of incidence from an initial incidence α_A to a transitory incidence α_B which remains constant whilst the wing is moving; finally, a return to the initial incidence occurs when the wing comes to rest.

Specification of a time scale involves two non-dimensional parameters depending on the time t measured from the start of the plunge and the stream velocity. A local non-dimensional time, $\lambda(\equiv Ut/x)$, refers to a cross-flow plane at a distance x from the apex, whilst a general non-dimensional time, $\mu(\equiv Ut/c_0)$, relates to the wing as a whole. It will be noted that the change in incidence from α_A to α_B is accompanied by a change in the resultant stream velocity from U to $(U^2+W^2)^{\frac{1}{2}}$. The additional component has, however, been ignored in the calculations of non-dimensional time. Owing to the size of the plates and the large incidences used, the effects of wall interference on the flow are likely to be appreciable. It should be realised that, although during a constant velocity plunge a steady incidence is applied, the wall interference effects will be varying with time because the plate is moving relative to the tunnel. In the experiment, the period for which the steady transitory incidence persisted was sufficient for the flow over the plate to have reached a state which, apart from the effects of tunnell-wall interference, could be regarded as steady.

4. *Presentation of Results.*

Most of the quantitative data were obtained for changes from zero to positive incidence, for which the conditions are listed in Table 1A and the non-dimensional spanwise positions $\eta = y/s$ and height $\zeta = z/s$ of the vortices are plotted against local non-dimensional time in Figs. 6 to 15. The scatter in the time histories of the vortex co-ordinates shown in these figures can be mainly associated with uncertainties

in the visual estimation of the vortex centres. The curves shown in the figures correspond to 6th order (full line) and 7th order (dashed line) Chebychev polynomials calculated to fit the displayed points. In Fig. 12 no experimental points are shown for $\lambda < 0{\cdot}4$ because for this case, ($x = c_0$), the leading edge of the plate was beyond the field of the camera. Fig. 16 shows the vortex position after the plunge has stopped, the positions of the mean curves having been estimated visually.

Table 1B lists three conditions in which particle observations were made at $x = 2c_0/3$ for plunges from a non-zero initial incidence of the 40° plate (i.e., the model of apex angle 40°). The photographic observations in these cases involved considerable re-arrangement of the optical system with consequent distortions and loss of accuracy; they have therefore been regarded as only of qualitative value and, although used in the discussion, are not presented in the same detailed form as the experiments listed in Table 1A.

5. *Discussion of Results.*

Discussion of the observations and measurements is divided into four sections dealing respectively with step-changes of incidence from zero to a positive value, from positive value to zero, and increase and decrease of incidence between positive values. The flow behaviour associated with the first type of change is described in some detail by the measurements, but the flows for the other kinds of step-change are described only qualitatively. Indeed, the transient flow for the first type of change only can be said to be reasonably well understood whilst the flow behaviour for the other changes involves more complicated processes which are difficult to visualize and to describe.

5.1. *Zero to Positive Incidence.*

Before detailed discussion of the measurements, it may be useful to consider the general nature of the three-dimensional flow field. Fig. 17a represents the condition occurring very shortly after the start of the plunge when the flow has separated along the leading edges and the free vortex layers are beginning to roll up and to form discrete vortices. These incipient leading-edge vortices combined with the vortex shed from the trailing edge form a closed vortex loop the rearward position of which is being continuously convected downstream. The diagram indicates only the existence of some form of closure of the loop. In reality, the portion of the loop associated with the tips of the wing would be rapidly distorted; generally, the vorticity contained in all portions of the vortex layers would suffer the combined effects of distortion and diffusion.

Fig. 17b depicts the condition at a rather later time when the flow in the neighbourhood of the wing is approaching a steady condition. Above the wing, the separation surfaces from the leading edges and the developing vortices are well defined; in the diagram for clarity they are shown only ahead of a particular cross-flow plane. The point of intersection of the vortex axis with the cross-flow plane is indicated in the diagram and will be referred to as the 'vortex centre' in the following discussion. Also indicated in the diagram is the path which the vortex centre has followed in this plane. It is the time history of the vortex centre along this path which forms the subject of the measurements.

Examination of the photographic records for all the plunges in which the initial incidence is zero shows that a vortex first appears close to the leading edge and then, with increasing height, moves inboard over the plate.

Consideration of the mean curves of Figs. 6 to 15 leads to the general conclusion that the movement of the vortex centre with respect to the plate is almost completed when the local non-dimensional time λ reaches 1·0, which corresponds to the time required for the free stream to travel from the apex to the cross-flow plane.

Figs, 18, 19 and 21 to 26 have been prepared from interpolated experimental data obtained from the mean lines of Fig. 6 to 15. In discussing these results it would be an advantage to be able to compare the vortex position at any time during the plunge with a steady-state position for the same value of incidence. Unfortunately, the condition obtained with a fixed model set at a steady incidence would not correspond exactly with the plunging condition because of differences in wind-tunnel interference that cannot be adequately assessed.

5.1.1. *Transient shape of vortex over the wing* (40° *plate*, $\alpha_B = 12{\cdot}4°$). The transient shapes of the vortex axis can be deduced from the measurements at the three cross-flow planes $x/c_0 = 1/2$, 2/3 and 1 which are collected together in Fig. 18. This diagram shows that the time histories for the vortex centres at each of the three stations are similar, but there is a tendency for the height of the vortex in approaching its steady value to be more delayed for the trailing-edge plane than for the other cross-flow planes.

Fig. 19 shows the plan and elevation positions of the vortex axis at various times $\mu(\equiv Ut/c_0)$ after the start of the plunge, whilst comparison with the theoretical results of Dore[4] is provided by Fig. 20 and will be referred to again in Section 5.1.4. These diagrams show that, at any instant of time, $\mu < 1{\cdot}0$, the vortex axis has reached its final position over a forward portion of the wing whilst still moving over a rearward portion. In both diagrams, the final position of the vortex appears as an envelope of the transient shapes. Furthermore, as shown in Fig. 20, in theory we can specify a travelling demarcation-point P (moving downstream with velocity U) ahead of which the vortex has reached its final position and downstream of which the vortex is still moving laterally. Whilst Fig. 19 shows generally similar transient configurations for the vortex axis, the measurements are unable to yield precise positions for the demarcation point between the final and steady positions. It will be noted that as the vortex moves away from the edge, there is a tendency for that portion of the axis which had not yet achieved its final steady-state position to remain parallel to the edge whilst that portion which has reached its steady position lies approximately along a ray through the apex. The interpretation of these observations is aided by the following simple approach involving a consideration of the behaviour of the fluid elements making up the vortex axis.

With reference to the figure below, which shows the leading apex of a delta wing, we consider the

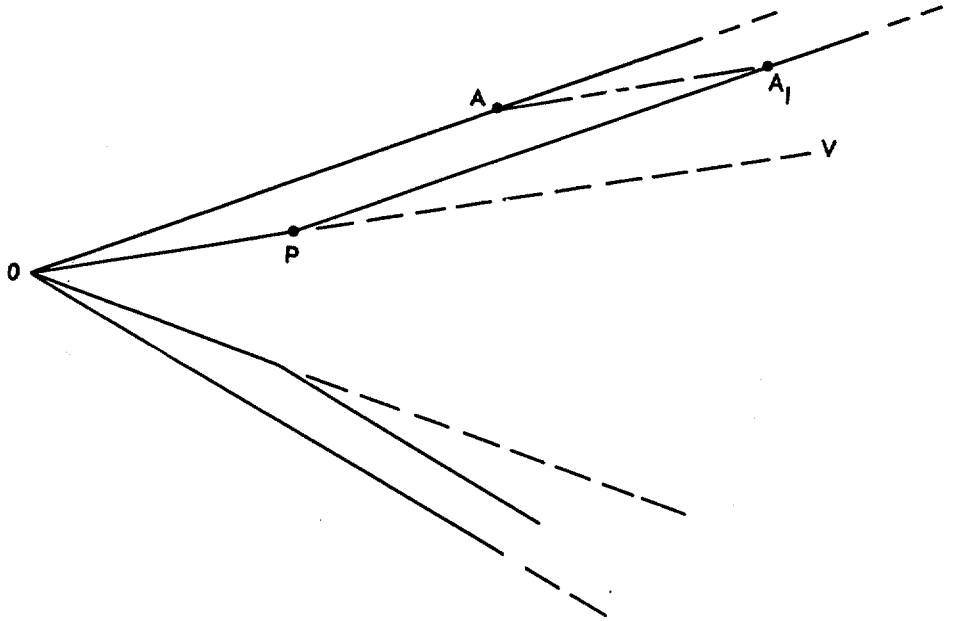

fluid particles that are in contact with the portion of the leading edge OA at the instant $t = 0$, when the incidence is changed. It seems plausible to assume that these particles will be the first to separate from the edge and thus that these same particles will at some later time form a portion PA_1 of the central axis of the complete vortex. It may also be assumed that the forward part of this vortex OP will be formed by those particles which have wetted the apex (i.e., a filament line through the apex). We consider each of these two groups of particles (i.e. the edge particles at $t = 0$ and the apex particles for $t > 0$) to be convected in the direction of the steady-state axis of the vortex, OV, with a uniform velocity which is of the same order as the stream velocity. Then, as shown in the diagram, the instantaneous shape and position of the vortex OPA_1 will bear some resemblance to those measured to the extent that over the forward region of the wing the vortex axis coincides with its steady state position, whilst to the rear

the initial vortex is being convected downstream and remains parallel to the leading edge. Also, for any cross-flow plane the time required to reach the steady state is the time taken to convect fluid from the apex.

However, this simple scheme is not entirely consistent with the observations because of the time-wise non-linear variations in both height and spanwise positions of a vortex centre.

5.1.2. *Locus of vortex centre in cross-flow plane.* The results for section $x/c_0 = 2/3$ for each of the three plates are used to derive the diagrams in Figs. 21, 22 and 23 which show the paths in a cross-flow plane after the plunging motion is applied. These paths have been obtained from the experimental mean lines for values of $\lambda = 0{\cdot}25, 0{\cdot}50, 0{\cdot}75, 1{\cdot}0$ and $1{\cdot}5$, the latter value being regarded as a reasonable approximation to a steady condition. Broken curves have been sketched through the points for $\lambda = 1{\cdot}5$ and joined to the point corresponding to the leading edge to indicate the general shape, as found in other experiments, of the line connecting the vortex positions for steady conditions over the range of incidence $0 < \alpha < \alpha_B$.

It is seen that for any given value of α_B the locus for the step-change of incidence applied in the experiments differs from that which would be obtained for a quasi-static, or very slow increase of incidence, as shown by the broken line. The locus for some intermediate rate of change from zero to α_B (i.e. a change less abrupt than a step-change) would be expected to lie between the broken and the full curves. Although there are no measurements of the transient positions very close to the leading edge, it is clear from the shape of the curves that the initial rate of change of vortex height with spanwise position, $(d\zeta/d\eta)$, is much greater for a step-change than for a quasi-static variation of incidence.

5.1.3. *Influence of incidence and aspect ratio.* Broadly speaking, the results show that the movements of the vortex centres are similar for the three plates and for various changes of incidence. Some differences of detail are present in the results but their true significance is obscured by uncertainties in the measurements. Although there is no conclusive evidence of any great sensitivity to change of aspect ratio, there is some evidence, for instance in Fig. 24, of a comparatively quicker initial approach to the steady position with larger changes of incidence. This effect is coupled with an increasing tendency for the vortex to overshoot and then return to its final position (e.g. Figs. 6b and 9b). In the real situations which are in some way analogous, such as an aircraft flying into a gust or during a manoeuvre, the incidence changes are usually very much less than those of the present experiment. The foregoing effects of large amplitude changes are therefore likely to be of academic interest only.

The unifying influence of the parameter α/k, which involves both incidence and aspect ratio, is discussed in the following Section.

5.1.4. *Comparison with theoretical calculations.* Following the initial observations of Ref. 3 and the tentative conclusion regarding the time taken for the vortex centre in each cross-flow plane to reach its steady position, Dore developed a theoretical treatment in Ref. 4 for a slender delta wing of infinite chord under transient conditions. In this treatment the flow at any chordwise position (x = constant) reaches its steady condition in time x/U. For any time $t < x/U$ the transient condition of the flow at each chordwise position is derived using an analogy between the unsteady condition and a related steady flow. In the application to a sudden change of incidence from zero to α, the analogous steady flow is that for a trapezium (truncated-delta) wing at uniform incidence α. Using the theoretical approach of Brown and Michael[5] to calculate vortex strength and position for the steady flow over the trapezium wing, Dore obtained these quantities as functions of only λ and α/k, where $k = \tan \varepsilon$.

Before making comparisons between the theoretical and experimental results, it must be emphasized that the Brown and Michael model gives steady vortex positions which are in considerable disagreement with observations, the calculated positions being too far outboard. However, the theoretical predictions of *the manner* in which the steady position is reached are conveniently compared with the observed path by reference to normalized displacements of the vortex centre from the edge:

$$H(\lambda) = (1-\eta)/(1-\eta_F),$$

$$Z(\lambda) = \zeta/\zeta_F$$

where η_F and ζ_F correspond to the final, or steady, position. Comparison with experimental observation can be made in a number of ways. Dore's theoretical calculations have been used to provide Fig. 20 which is comparable with the experimental diagrams of Fig. 19. For this purpose, the calculated time-wise movement of the vortex centre $H(\lambda)$ and $Z(\lambda)$ have been combined with the measured 'final' positions corresponding to $\lambda = 1{\cdot}5$, to give calculated instantaneous shapes of the vortex axis that must agree with the measurements for the steady condition. The calculations have been made for a value of α/k of 0·564 whereas the experimental results are derived within the range $0{\cdot}58 < \alpha/k < 0{\cdot}60$; however the values of $H(\lambda)$ and $Z(\lambda)$ are shown by the theory to be insensitive to this parameter.

The comparison between experiment and theory, Figs. 19 and 20, shows close agreement for the plan positions of the vortex core for the same values of μ. Although the theory imposes a uniform axial speed for the point P at which the vortex core coincides with its final position, it clearly predicts the decelerating inboard movement of the vortex core found by experiment. Agreement between experiment and theory is not so close regarding the shape of the vortex in side-elevation.

To examine the theoretically predicted unifying role of parameter α/k, comparison is made in Fig. 25 between the results for those plunges with the three different plates that have approximately the same value of α/k (i.e. 0·53, 0·60, 0·56, experiments 3, 6 and 9). It is seen from this figure that the time histories of the height of the vortex centre agree reasonably well, but that the curves for the spanwise position do not collapse because of a disagreement in the final positions. In Fig. 26 the movements are normalized with respect to the final positions and are compared with the results of the theoretical calculations made for approximately the same value of α/k. The observed spanwise movements of the vortex collapse reasonably well to a single curve but they disagree with the theory by showing additional motion when $\lambda > 1{\cdot}0$. The observed height parameter, $Z(\lambda)$, collapses less well but is in general agreement with the theory.

The general appearance of Figs. 21 to 23 is similar to the corresponding diagram of Dore shown in Fig. 3 of Ref. 4 which shows similar distinctions between the full and broken curves.

5.2. *Positive to Zero Incidence.*

A step-change of incidence from a positive value to zero was obtained in two ways:

(a) by the cessation of the plunging motion of a wing which, when stationary, had been set at zero incidence,

(b) by the application of a reverse plunge with velocity selected to neutralize an initial positive incidence of the wing.

All the observations and measurements were made with the 40° plate. Measurements of the movement of the vortex centre at the 2/3 chord position following the cessation of a plunge equivalent to an incidence of 12·6° are shown in Fig. 16. In these diagrams, λ now denotes the local non-dimensional time after the plunge has ceased. It will be noted that the vortex height does not appear to reduce immediately the plunge ends, there being a delay in this movement at least until $\lambda = 0{\cdot}2$. On the other hand, no similar delay in the start of the inboard movement of the vortex centre is observable. Unlike the case of step *increase* in incidence, the vortex components in a cross-flow plane following the loss of incidence become weaker and after a certain time the vortex centre can no longer be located. Because of this, measurement of vortex centre positions in these particular experiments was not possible for $\lambda > 0{\cdot}6$.

Other evidence of the general nature of the flow change was obtained under condition (b) from an examination of the behaviour of a sheet of dye issuing from a leading edge. Fig. 27 shows successive photographs of a section of this sheet approximately at mid-chord position. Four photographs are shown, the first corresponding to a time just before the reverse plunge starts, the other three corresponding to successively later times after the plunge has started. After the incidence changes to zero, the sheet becomes closer to the surface, the position of the vortex centre moves inboard and downwards and the apparent strength of the vortex is reduced. It is clear from these photographs that attachment at the leading edge does not occur immediately incidence is reduced, but that separation persists probably because of the induced velocity associated with the continuing presence of the vortex system.

No information was obtained of the transient behaviour in the wake of the wing for this type of motion, and no attempt will be made to speculate on this aspect of the flow. However, for the region above the wing, the transient flow after the incidence has been reduced to zero is schematically illustrated in Fig. 28 which shows the vortex system that existed above the wings when $\lambda < 0$ to have been convected bodily downstream. Under the initial steady conditions, due to the action of the feeding vortex sheets the strength of each of the vortices increases with distance from the apex, and it is considered that this distribution of vortex strength would continue to be attached to the vortex system whilst it is being convected over the wing. Thus, on this assumption, as the observations show, any particular cross-flow plane would experience a vortex which, with increasing time, appears to move inboard and downwards whilst decreasing in strength.

5.3. *Positive to Higher Incidence.*

Observations of dye and particle tracks in cross-flow planes have been used to construct the schematic three-dimensional representation of Fig. 29, which shows the general shape of the leading-edge vortex layer when a plate whose initial positive incidence of 11° is effectively doubled by the plunge motion. The most noticeable feature in this case, shown by the cross-section diagrams included in Fig. 29, is the generation of a second vortex which, first appearing close to the leading edge at the commencement of the plunge, moves inboard with increasing strength and increasing influence over the whole flow field; it finally becomes established at a position higher above the plate than that occupied by the original vortex. Soon after the inception of the second vortex, the vortex flow related to the initial condition is noticeably affected: whilst becoming weaker, its centre is induced to move in a circular path under the new vortex. The dye photographs of Fig. 30, although pertaining to a somewhat smaller change of incidence, serve to illustrate the main features which have been described; in addition, some progressive modification to the shape of the secondary-flow region between the main vortex flow and leading edge is also made visible by the dye.

With regard to the three-diamensional convolutions of the vortex layer which are suggested in Fig. 29, it is difficult to imagine the precise way in which the sheet remains continuous between stations (a) and (b). However, other features such as the convection of the distortion in the vortex layers associated with the second vortex are probably representative of the real flow and are borne out to some extent by the manner in which vortex flow forms from an initial zero incidence (Figs. 19 and 20) as mentioned in Section 5.1.1.

The incidence changes that were made to obtain these observations have all been large (approx. 11°) and produced easily observable second vortices. For smaller changes of incidence, the strength of the second vortex would be expected to be reduced in proportion and it would not be such a significant feature of the flow.

5.4. *Positive to Lower Positive Incidence.*

When a reverse plunging motion applied to a plate already at positive incidence results in a lower effective positive incidence, no rapid or large changes in the shape of the rolled-up vortex layers are immediately apparent. Fig. 31 represents the changes of shape of a layer as observed in the cross-flow plane for a step function change from $\alpha_A = 22$ deg. to $\alpha_B = 11$ deg. As for a change of steady incidence in this range, the initial and final vortex-centre positions are changed mainly in height only, but there is some evidence during the transition period of an initial inboard movement of the vortex centre followed by an outboard movement to its final location. The initial behaviour of the vortex is qualitatively as if $\alpha_B = 0$.

6. *Speculations on the Transient Lift and its Distribution.*

Before discussing the possible form of the transient lift distribution for a delta wing with vortex flow, it is useful to refer briefly to existing information on indicial aerodynamics of wings in general. Theoretical treatments (*see* for instance Ref. 6 and 7), when applied to wings in subsonic flow without leading-edge

separation, indicate that the time history of the lift following a sudden plunge has the general form shown in Fig. 32 in which the proportion of the final steady lift is plotted as a function of the time after the start of the plunge. This time history shows two features, (a) a sharp pulse at time $t = 0$ followed by (b) the Wagner effect, a more gradual variation with asymptotic approach to the final value. The pulse can be associated with the concept of a mass of fluid, the virtual mass, attached to the wing and subjected to the very high acceleration at the start of the plunge. For a gradual start to the plunge or with compressibility present, the pulse would be less intense and extend over a finite time. For a perfect step-change in incompressible flow the pulse corresponds to a Dirac impulse; linear theory states that its effects have disappeared for $t > 0$, however small. Apart from the pulse, the initial value of the lift (i.e. for $t = 0+$) is shown by theory to be 0·5 times the final lift in the case of a two-dimensional wing and to tend towards the steady value as the aspect ratio decreases towards zero.

Although the approach to a steady condition is strictly asymptotic, for most purposes this condition can be regarded as having been attained when the lift has reached some arbitrarily chosen proportion, say 95 per cent, of the final value. Linear theory indicates that such a condition would be reached in a streamwise distance of some 12 chords for a two-dimensional wing and in shorter distances for wings of smaller aspect ratio. Linear slender-wing theory leads to the conclusion that the lift develops instantly.

It seems that, in the present case of the sharp-edged delta wing, it should be possible to associate the variation of lift for $t > 0$ with the development and convection of the vortex system following the start of the plunge. If this is so, we can then attempt to deduce a lift distribution based on steady, or quasi-steady, considerations from the observed transient flow behaviour. Although the following discussion is to a large extent intuitive and speculative, some support for the approach derives from an empirical conclusion, discussed in Ref. 8 that, in the presence of leading-edge vortices, an instantaneous spanwise pressure distribution during unsteady conditions can be closely matched with a pressure distribution for an equivalent steady condition. The following speculations are made on the assumption that a major proportion of the pressure field can be associated with the presence of the leading-edge vortices and in the knowledge that, under steady conditions, the upper surface pressure distribution includes, along a line from the apex, a ridge of high suction almost directly beneath each vortex. The following discussion and Figs. 33 and 34 refer to changes that would occur in the typical spanwise distribution of the lift for an infinite flat-plate delta wing. In practice, as well as the suction peak already mentioned, the spanwise distribution would contain a plateau (or second peak) corresponding to the region of secondary separation on the upper surface close to the edge. For simplicity in showing the character of the time-wise variations, this feature has been omitted from the diagrams by smoothly fairing the curves between the edge and the main suction peak.

In each diagram, the initial steady distribution of sectional lift is designated $\lambda < 0$, whilst the final steady distribution, assumed for practical purposes to be achieved when $\lambda \simeq 1{\cdot}0$, is designated $\lambda > 1$. The transient distributions, for successive intermediate times λ_1 and λ_2 are derived from knowledge of the cross flow on a quasi-steady basis. In other words, the instantaneous lift distribution is that which would be associated with a steady flow corresponding to the actual instantaneous vortex positions.

For an increase of incidence from zero, in Fig. 33a, we would expect the initial development of the vortex flow to be accompanied by a load distribution with a peak first appearing close to the leading edge and then moving inboard to its final steady position. It is known from the observations that for any given spanwise section during the transient phase, the strength of the vortex grows and the height above the surface increases. Since the magnitude of the suction acting at the wing surface depends on the strength and proximity of the vortex, it is plausible to suggest that the height of the peak will increase rapidly at first and that the peak will later broaden with the approach to the steady condition.

When incidence is reduced to zero, the flow observations clearly indicate that the same transient changes do not simply occur in the reverse direction. As shown in Fig. 33b, we should expect the peak in load distribution to decrease in magnitude whilst moving further inboard. It follows that the pressure change at any given position on the upper surface of the wing is not necessarily reversible with respect to increasing and descreasing incidence. For instance, following an increase of incidence, a position close to the leading edge would experience a rapid rise in loading to a maximum with a subsequent decrease; on the other hand, following a decrease of incidence to zero, the loading at this point would be expected

to fall monotonically. This irreversibility of the pressure variations is of interest in connection with the difference found by Roberts and Hunt (Ref. 2) between the effects of lift-increasing and lift-decreasing gusts on the pressure at a fixed point.

Figs. 34 a and b suggest the behaviour of the lift distribution when incidence changes from one positive value to another. As indicated in Fig. 34a, following an increase in incidence, the height of the original peak would be expected to increase only slowly at first whilst an additional distribution of lift appears outboard and moves inboard to augment the previous peak. On the other hand, subsequent to a decrease of incidence, Fig. 34b suggests that there would be a gradual decrease in the peak whilst it moved first inboard, then returned and eventually reached a slightly more outboard position.

It follows from the previous discussion that for an increase of incidence the sectional lift at any chordwise station will increase during the period $0 < \lambda < 1{\cdot}0$ and will reach its steady value when $\lambda = 1{\cdot}0$ approx and thus the total lift will increase during the interval $0 < \mu < 1{\cdot}0$ to reach its steady value when $\mu = 1{\cdot}0$ approx. Regarding the chordwise distribution of lift, we note that the further forward the station, the earlier it reaches its steady condition: this means that the centre of lift during the transient condition following an increase of incidence will be ahead of its steady position. By contrast, the transitory centre of lift after a decrease of incidence would be aft of the steady position.

The above speculations regarding the development of total lift are consistent with the results of linearized theory (Refs. 7 and 9) which, for a delta wing of aspect ratio 2 in incompressible flow, predicts that 95 per cent of the final lift will be acting after a travel of a chord length. On the other hand, the non-linear theoretical results of Dore (Ref. 4), using the mathematical model that has shown reasonable agreement with the experimental observations regarding the vortex behaviour (*see* Section 5.1.4), predicts a lift variation which is considerably different from the variation inferred above. Indeed, for values of α/k corresponding to those of the experiments, this non-linear treatment concludes that the lift would decrease from a large value for $t = 0+$, pass through a value some 4 per cent greater than the steady value for $\mu \simeq 0{\cdot}1$ and remain within 1 per cent of the final value for $\mu > 0{\cdot}2$. Thus we are faced with the surprising and unsatisfactory situation that our conjectures regarding lift development based on vortex flow observations are more in accordance with linear theory which ignores the leading-edge vortices than with the predictions of a theory which does take account of these features. The matter would obviously be clarified by measurements of transient lift but the practical difficulties would be considerable.

The indications from the present investigation can be compared with those of Hunt, Roberts and Walker (Refs. 1 and 2) who measured the behaviour of upper surface pressure at fixed points on a model delta wing subjected to a gust obtained by propelling the model across a jet of air. Their results suggest that the pressure due to a lift-increasing gust develops in the time taken to travel about 3 chords length, which is approximately three times as long as that indicated by the present experiments. On the other hand, the development time following a gust which decreases an initial lift to zero was found to be much less and reasonably consistent with the present results. That a difference should exist between the respective transient behaviour of the pressure at a fixed point after positive and negative gusts is fully consistent with the present conclusions regarding irreversibility. However, no explanation of the difference in the development times between an incidence-increasing *gust* and an incidence-increasing *plunge* can be offered apart from noting that, whereas the sudden plunge requires the convection of only a discontinuity in the vortex flow, a gust involves the convection of a change in local incidence as well. A conjecture that the convection of the two features would take longer than the one would be consistent with the difference between the present results and those of Refs. 1 and 2.

7. *General Conclusions.*

A general conclusion from the present experiments is that the vortex flow over a delta wing following a sudden plunge can be regarded as having reached a steady condition approximately in the time taken by the stream to travel one chord length. Also, we may conjecture that the total lift will reach its steady-state value in the same period of time.

With regard to the transient loading distribution, the experiments have indicated the manner in which, by a convective process, the flow at each spanwise station reaches its steady condition. For any given

station, the observed vortex movements, and hence the transient changes of loading, are not necessarily reversible with respect to increases and decreases of incidence.

The experimental results regarding the time necessary to achieve steady conditions lend support for the theoretical approach of Dore (Ref. 4) which is based on slender-wing theory. After certain allowances are made for known differences between theoretical predictions and measurements for steady conditions, the theory also shows reasonable agreement with the observed behaviour of a vortex centre in a cross-flow plane. However, when one considers the transient development of the aerodynamic loading, results based on the same theoretical treatment are at variance with the inferences from the flow observations.

With regard to future work directed to the problem of the slender delta wing encountering a gust, it would seem that the value of further qualitative work with step-changes of incidence is likely to be small. What is most urgently needed is more detailed information on pressure distribution and the lift force measured in a simulated gust.

LIST OF SYMBOLS

U		Free-stream velocity
W		Plunge velocity
c_0		Root chord
s		Local semi-span
ε		Semi-apex angle of delta plate
k	$\equiv$	Tan ε ($\equiv \frac{1}{4}$ aspect ratio)
α		Wing incidence
α_A		Incidence of delta plate before and after plunge
α_B		Incidence during plunge
t		Time measured after step-change of incidence
λ	$\equiv$	Ut/x, local non-dimensional time
μ	$\equiv$	Ut/c_0, general non-dimensional time
x, y, z		Co-ordinates fixed in the wing
η, ζ		Non-dimensional co-ordinates of the vortex centre
η_F, ζ_F		Co-ordinates of final position of vortex centre
$H(\lambda)$	$\equiv$	$(1-\eta)/(1-\eta_F)$ } Co-ordinates of vortex centre normalized with respect to η_F, ζ_F
$Z(\lambda)$	$\equiv$	ζ/ζ_F }

REFERENCES

No.	*Author(s)*	*Title, etc.*
1	G. K. Hunt, D. R. Roberts and D. J. Walker ..	Measurements of transient pressures on a narrow delta wing due to an upward gust. A.R.C. C.P. 624, September, 1961.
2	D. R. Roberts and G. K. Hunt	Further measurements of transient pressures on a narrow delta wing due to a vertical gust. A.R.C. C.P. 1012, April, 1966.
3	N. C. Lambourne, D. W. Bryer and J. F. M. Maybrey	A preliminary note on the behaviour of the leading-edge vortices on a delta wing following a sudden change of incidence. NPL Aero Note 1006. A.R.C. 24 187. November, 1962.
4	B. D. Dore	Non-linear theory for slender wings in sudden plunging motion. NPL Aero Report 1128. Aero Quart. 17.2 May, 1966. A.R.C. 26 488. December, 1964.
5	C. E. Brown and W. H. Michael	On slender delta wings with leading-edge separation. NACA TN 3430.
6	H. Lomax	Indicial aerodynamics. Chapter 6, Part II, Manual on Aeroelasticity AGARD.
7	B. D. Dore	The unsteady forces on finite wings in transient motion. R. & M. 3456, September, 1964.
8	N. C. Lambourne, D. W. Bryer and J. F. M. Maybrey	Pressure measurements on a model delta wing undergoing oscillatory deformation. NPL Aero. Report 1314, A.R.C. 31 979, March, 1970.
9	J. A. Drischler	Approximate indicial lift functions for several wings of finite span in incompressible flow as obtained from oscillatory lift coefficients. NACA TN 3639.

APPENDIX

Comparison of Several Types of Incidence Change.

Fig. 35 illustrates a number of fundamental ways in which the incidence of a wing can be altered suddenly from one value to another. Some of these are of interest in connection with the theoretical synthesis, on the assumption of linearity, of the effects of more general unsteady motions. Two of the changes, the sudden plunge and the instantaneous rotation in pitch, consist of step-function alterations of incidence, whilst the third involves entry into a sharp-edged gust. The class of change which occurs from an initial condition of zero lift also includes the fourth example of the diagram, the sudden start.

For a wing moving initially through a stationary medium, the sudden plunge can be considered to be a change in the flight direction but without the introduction of rotation in pitch: alternatively, it can be regarded as a suddenly applied downward rate of translation transverse to a moving stream. Instantaneous rotation in pitch involves no alteration in the translatory motion of the wing, but a change in the orientation of the wing. The sharp-edged gust is a plane front (or vortex sheet) beyond which the medium has an upward velocity component. Unlike the previous changes, the gust involves a spatial discontinuity in the medium.

Although a step-function plunge, pitch or start each lead immediately to similar steady motions and identical steady downwash distributions, kinematic differences between these various changes become apparent when the instantaneous distributions of downwash over the chord of the wing are considered. The sudden plunge needs a very high acceleration for a brief time to give a discontinuity in the downward velocity component but entails no discontinuity in displacement; the downwash is finite and uniform over the chord. The sudden start includes a discontinuity in forward velocity but, like the plunge, involves a uniform distribution of downwash. Instantaneous rotation about a pitching axis within the wing chord involves a discontinuity in angular displacement and requires a very large angular velocity for a short time during which the values of the downwash at leading and trailing edges are very large in magnitude and of opposite sign. Whereas for the plunge and pitch the changes of downwash occur instantaneously, the gust requires the passage of a spatial discontinuity in downwash and this takes a finite time to travel across the chord of the wing.

For all the cases that we are considering, the steady value of the lift resulting from the changes would be the same, but when the speed of motion is subsonic these values can only be approached asymptotically. In practice, however, interest is confined to the variation in lift that occurs very soon after a change and this must be dependent on the past history of the downwash distributions. As has been indicated, this is not the same for all the changes. Following the classical treatment of Wagner and Küssner regarding the development of lift for an aerofoil, the variation of lift following a sudden plunge or start is often referred to as the Wagner effect, whilst the lift variation following entry into a gust is referred to as the Küssner function.

TABLE 1

Experimental Conditions Investigated.

$U = 5$ ins/sec (0·13 *m/s*).

(A) *Changes from zero to a positive incidence* α_B

Experiment No.		1	2	3	4	5	6	7	8	9	10
Plate apex angle 2ε (deg.)		20	20	20	40	40	40	40	40	60	60
Chordwise position (x/c_0)		2/3	2/3	2/3	2/3	1/2	2/3	1	2/3	2/3	2/3
Plunge velocity W/U		0·45	0·21	0·09	0·44	0·22	0·22	0·21	0·15	0·34	0·21
Change of incidence $\alpha_B = \tan^{-1} W/U$ (deg.)		24·4	11·8	5·3	23·8	12·4	12·6	12·1	8·4	18·6	11·9
α_B/k (rad)		2·41	1·17	0·53	1·14	0·60	0·60	0·58	0·40	0·56	0·36
Vortex position	η (span)		0·64	0·68	0·64*	0·64	0·63	0·62	0·65	0·63	0·63
($\lambda = 1·5$)	ζ (height)		0·34	0·20	0·33*	0·20	0·21	0·20	0·16	0·21	0·16
Fig. No.		6	7	8	9	10	11	12	13	14	15

*extrapolated values

(B) *Changes from positive incidence* α_A *to positive incidence* α_B *40° plate,* $x/c_0 = 2/3$

Experiment No.	11	12	13
α_A (deg.)	11	11	23
α_B (deg.)	0	22	12

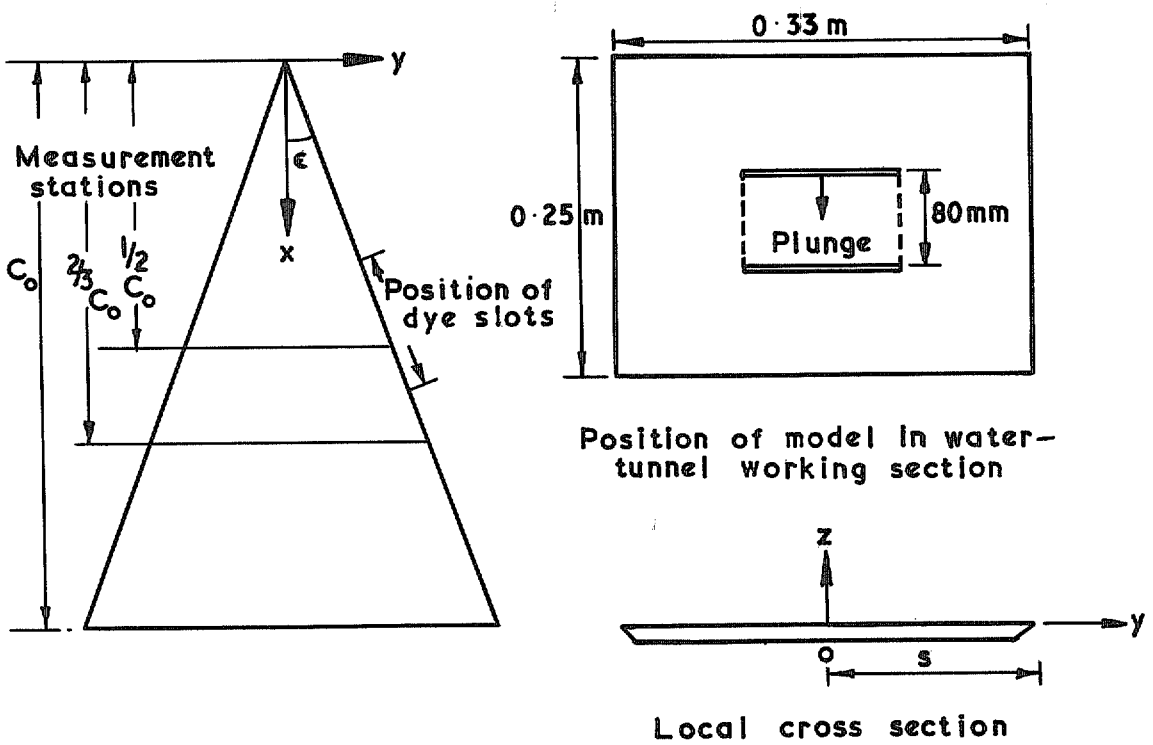

Dimensions of plates

Area of plate $0 \cdot 0115\ m^2$

Thickness $5 \cdot 0\ mm$

Chamfer angle normal to L.E. $19 \cdot 3^0$

Chamfer angle normal to T.E. $14 \cdot 0^0$

Wing apex angle 2ϵ (degrees)	20	40	60
Aspect ratio	0·705	1·456	2·310
Chord C_o (m)	0·255	0·178	0·141
Semi-span at T.E	0·045	0·065	0·082

FIG. 1. Reference system and dimensions of plates and tunnel.

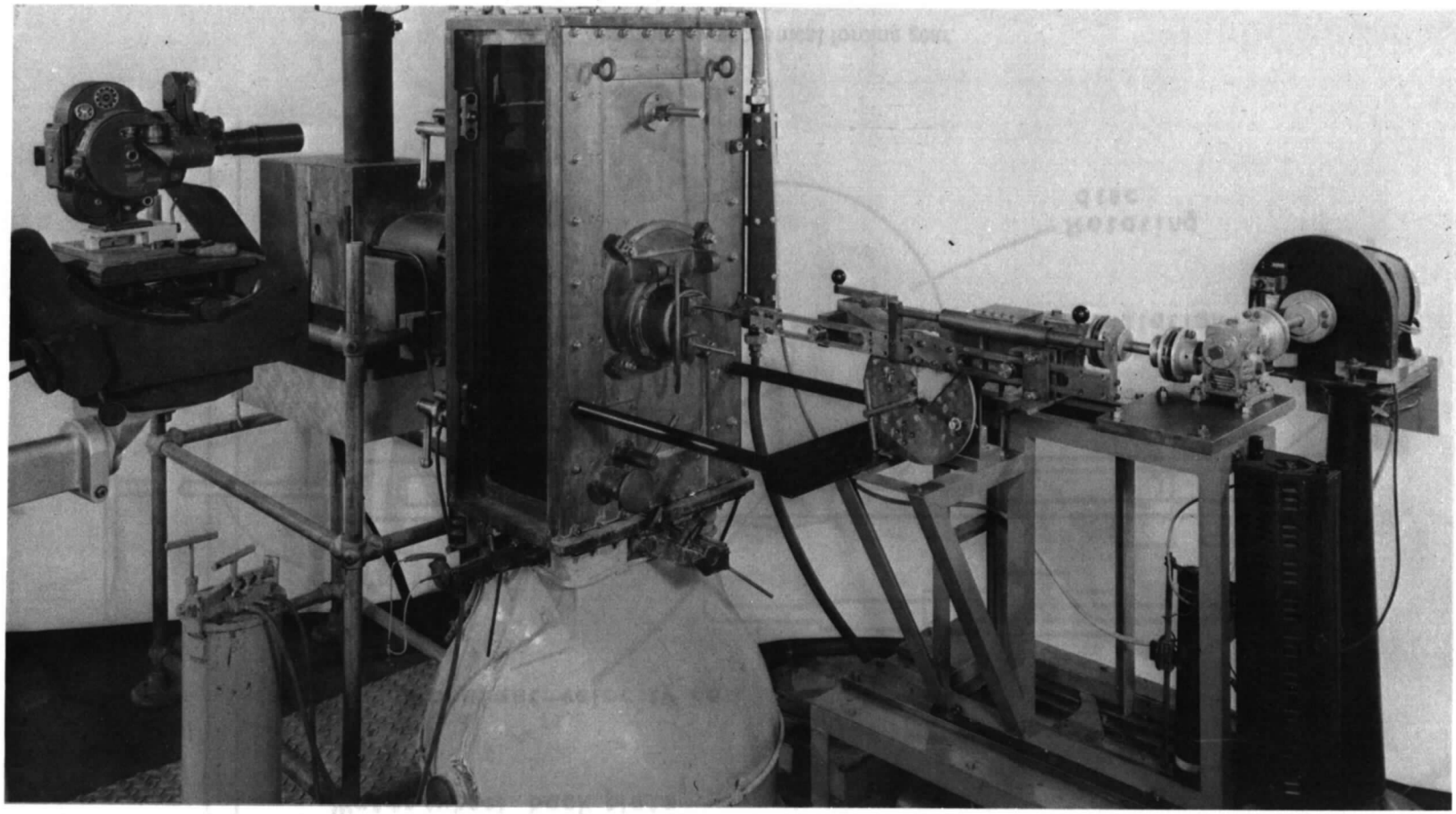

FIG. 2. Arrangement of apparatus around water-tunnel working section.

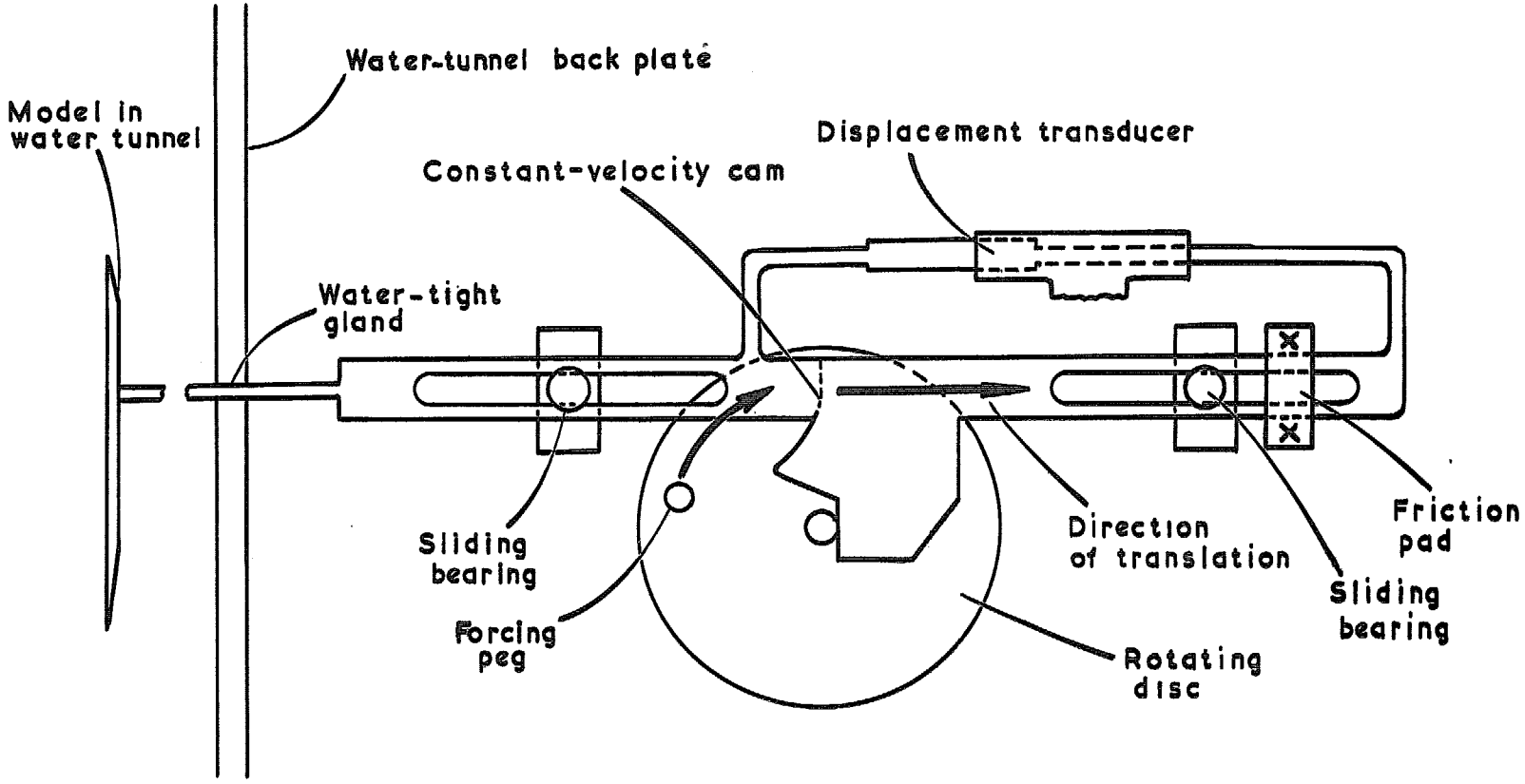

FIG. 3. Diagram of mechanical forcing gear.

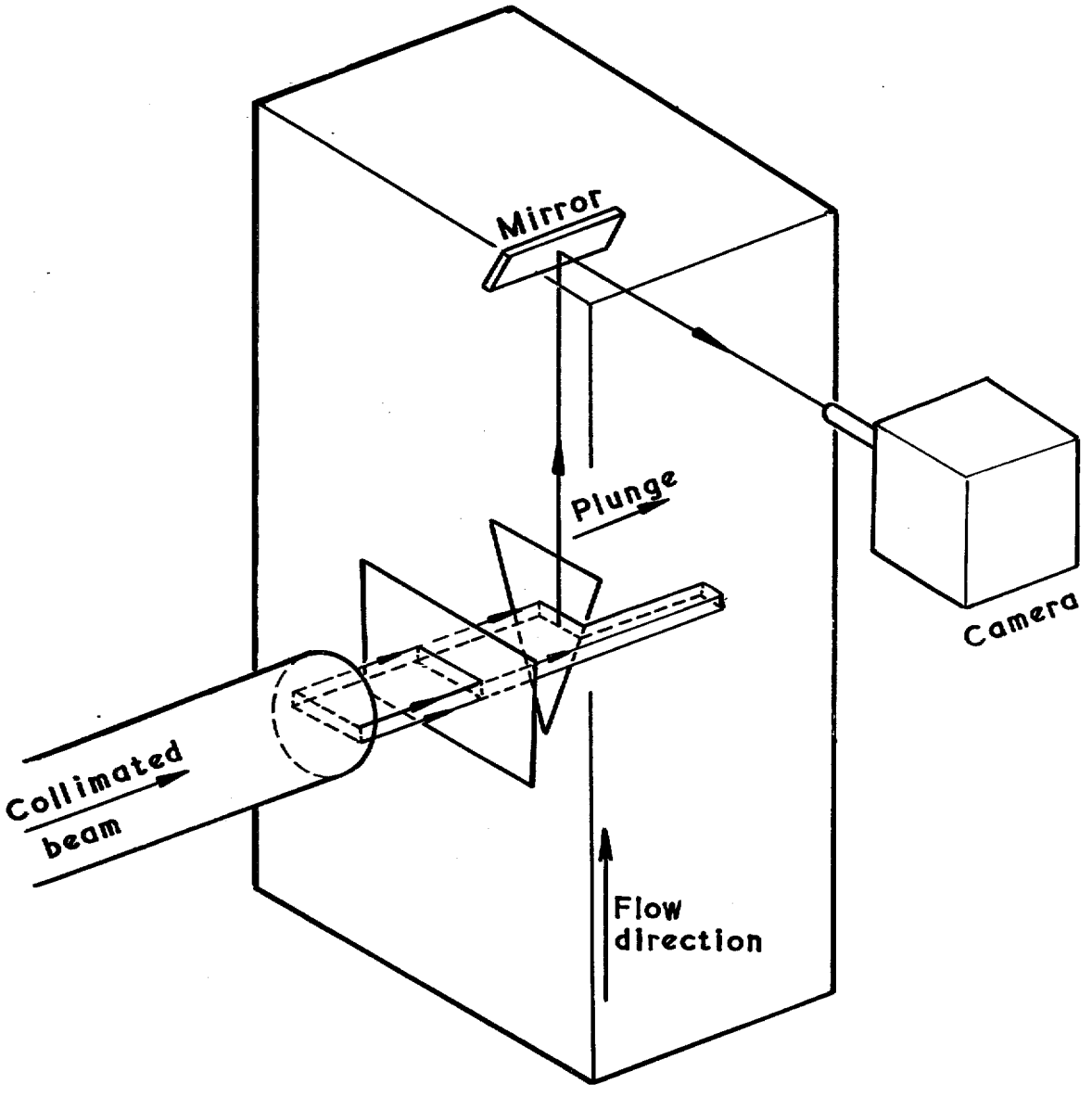

FIG. 4. General arrangement for filming cross-flow planes.

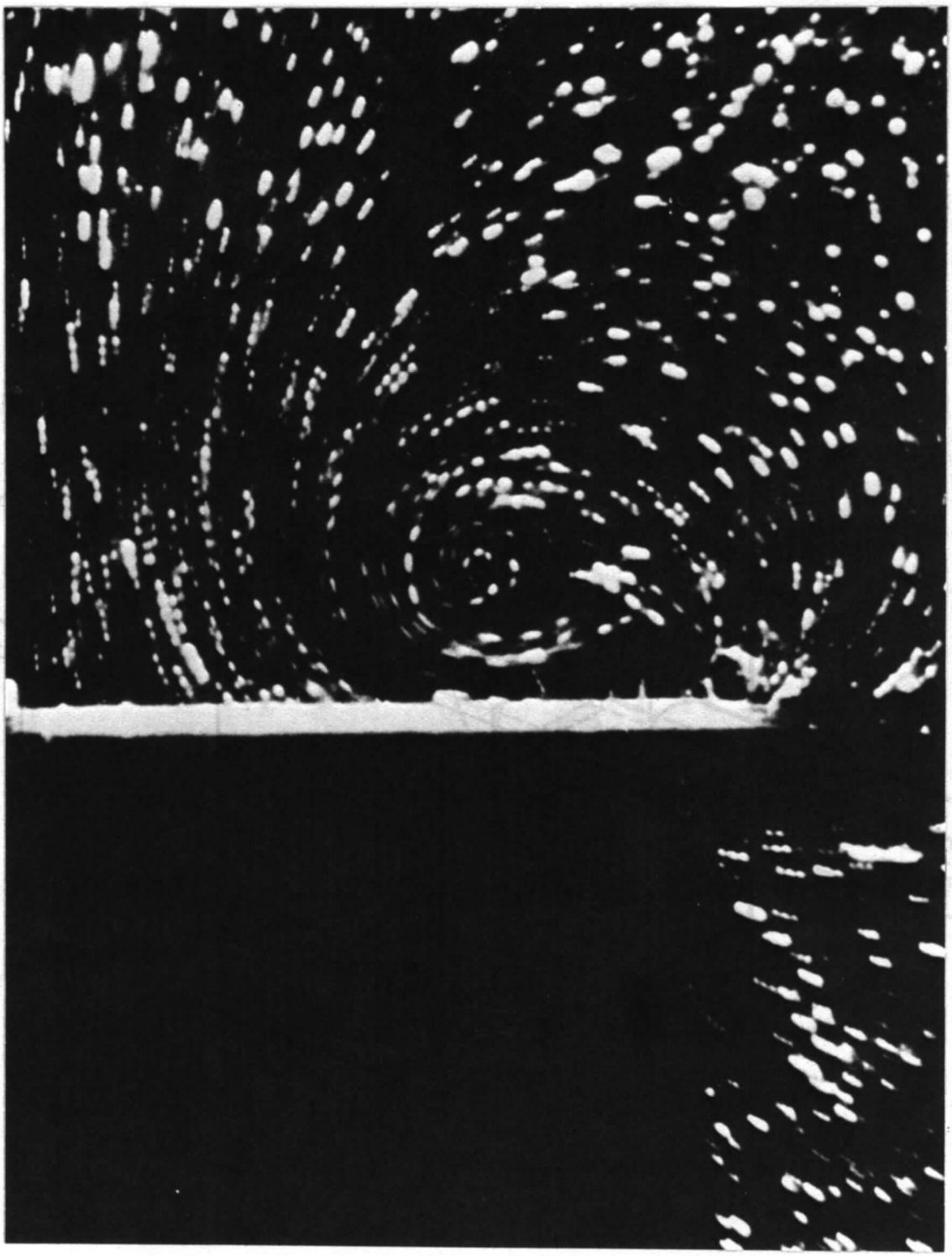

FIG. 5. Typical ciné-frame of cross-flow field.

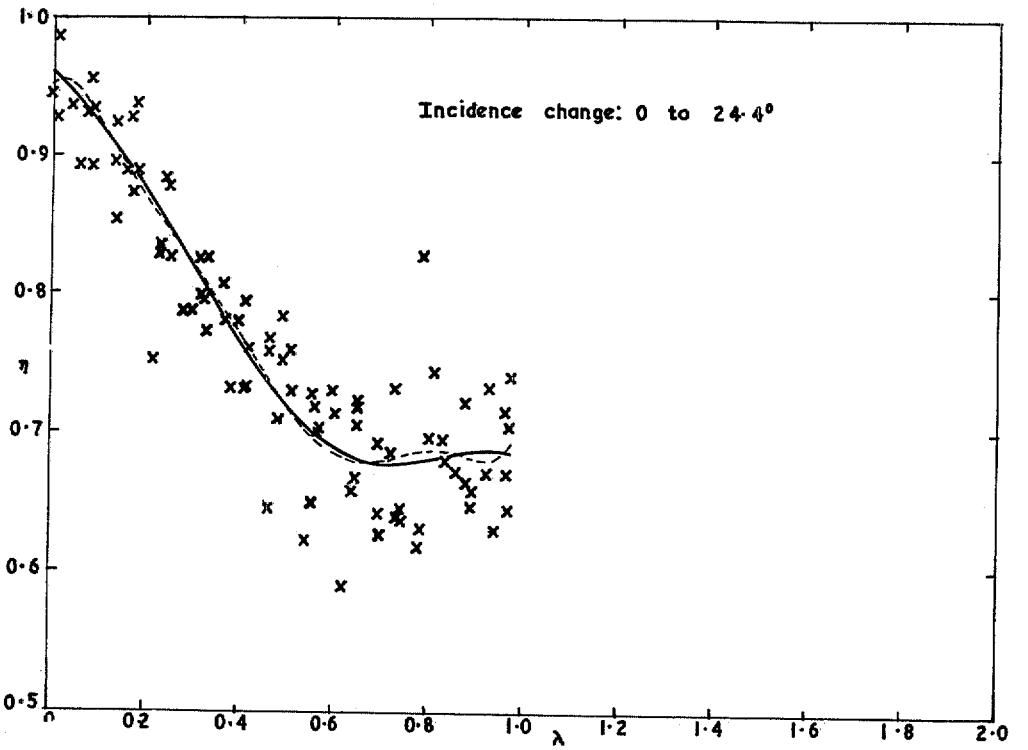

FIG. 6a. Expt No. 1. Spanwise position of vortex centre for 20° plate $x/c_0 = 2/3$.

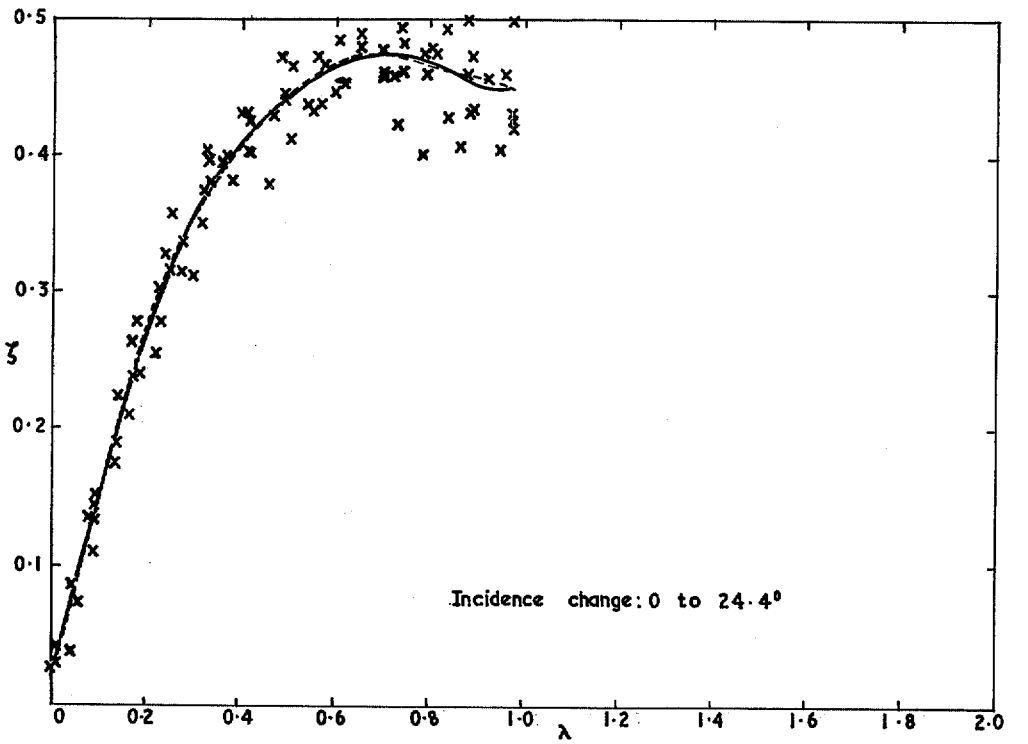

FIG. 6b. Expt. No. 1. Height of vortex centre above 20° plate $x/c_0 = 2/3$.

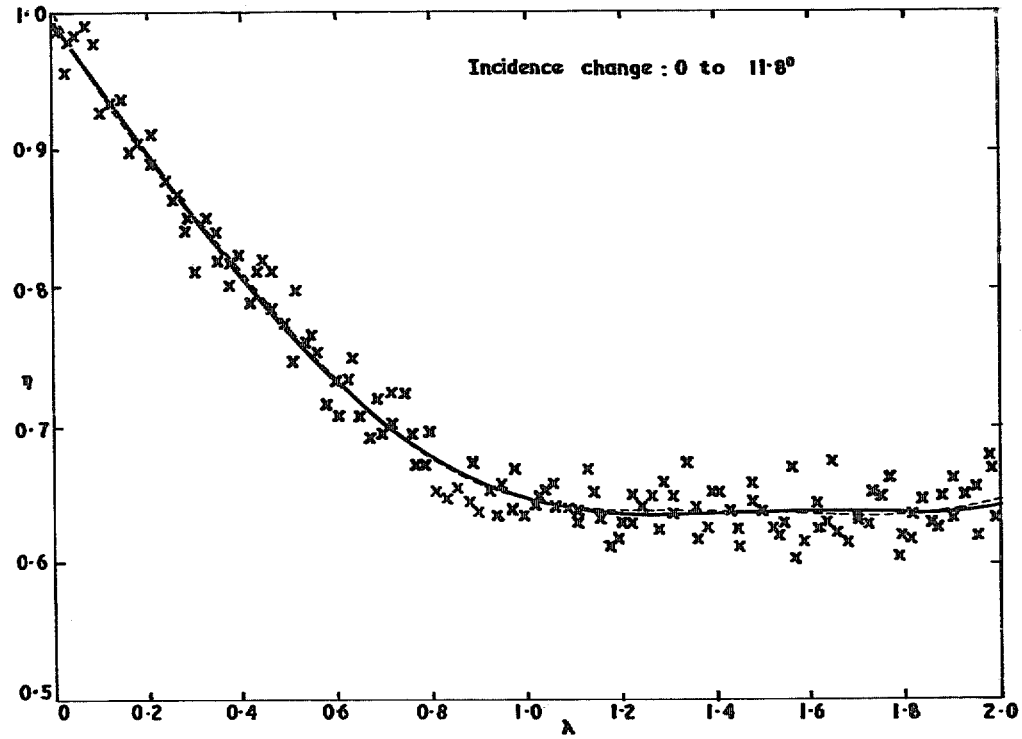

FIG. 7a. Expt. No. 2. Spanwise position of vortex for 20° plate $x/c_0 = 2/3$.

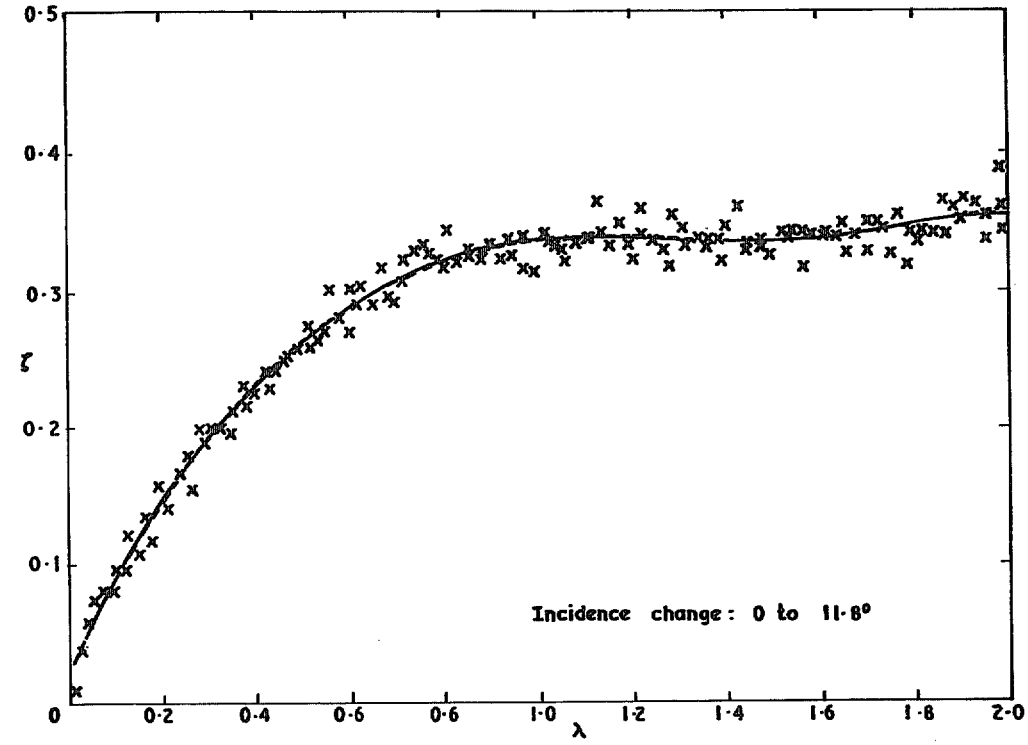

FIG. 7b. Expt. No. 2. Height of vortex centre above 20° plate $x/c_0 = 2/3$.

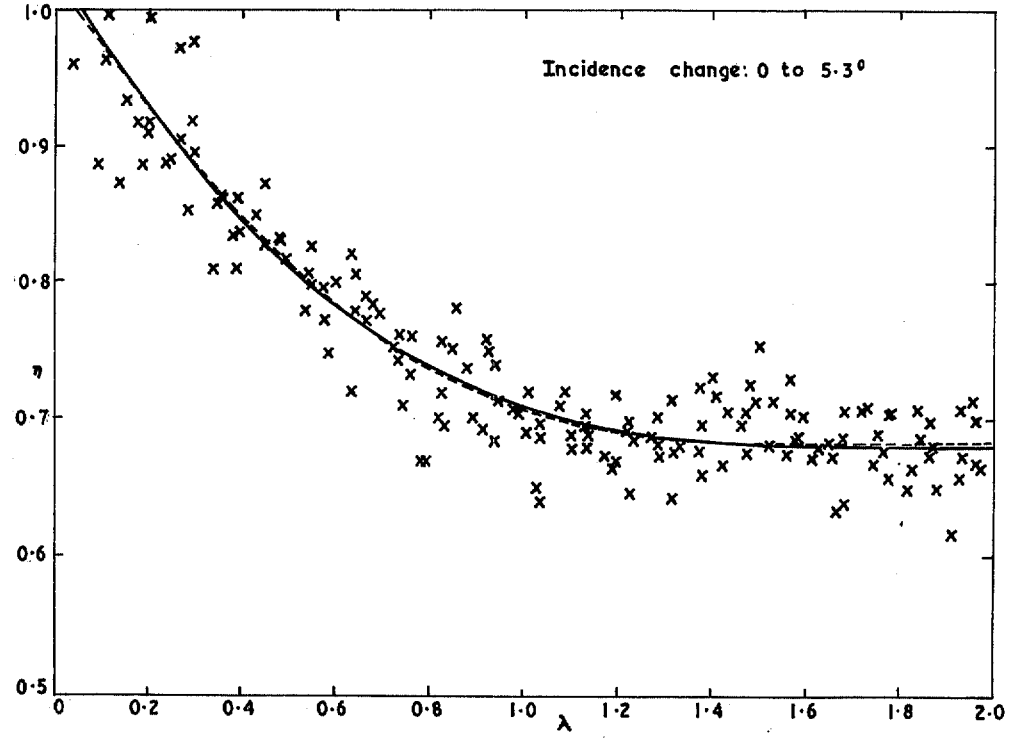

FIG. 8a. Expt. No. 3. Spanwise position of vortex centre for 20° plate $x/c_0 = 2/3$.

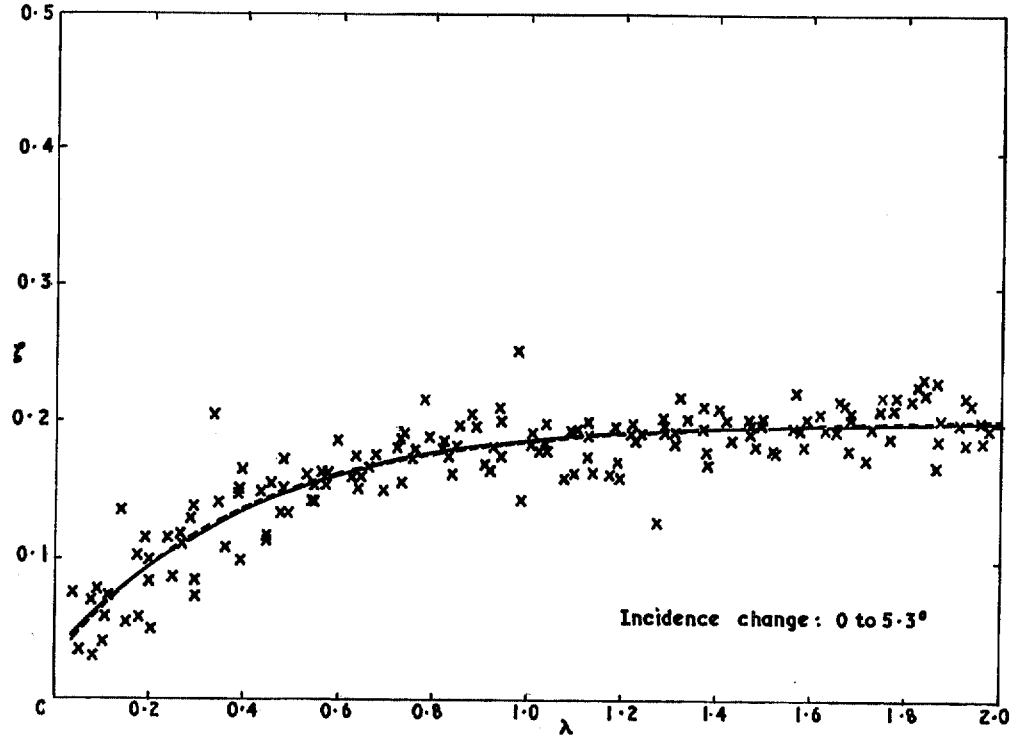

FIG. 8b. Expt. No. 3. Height of vortex centre above 20° plate $x/c_0 = 2/3$.

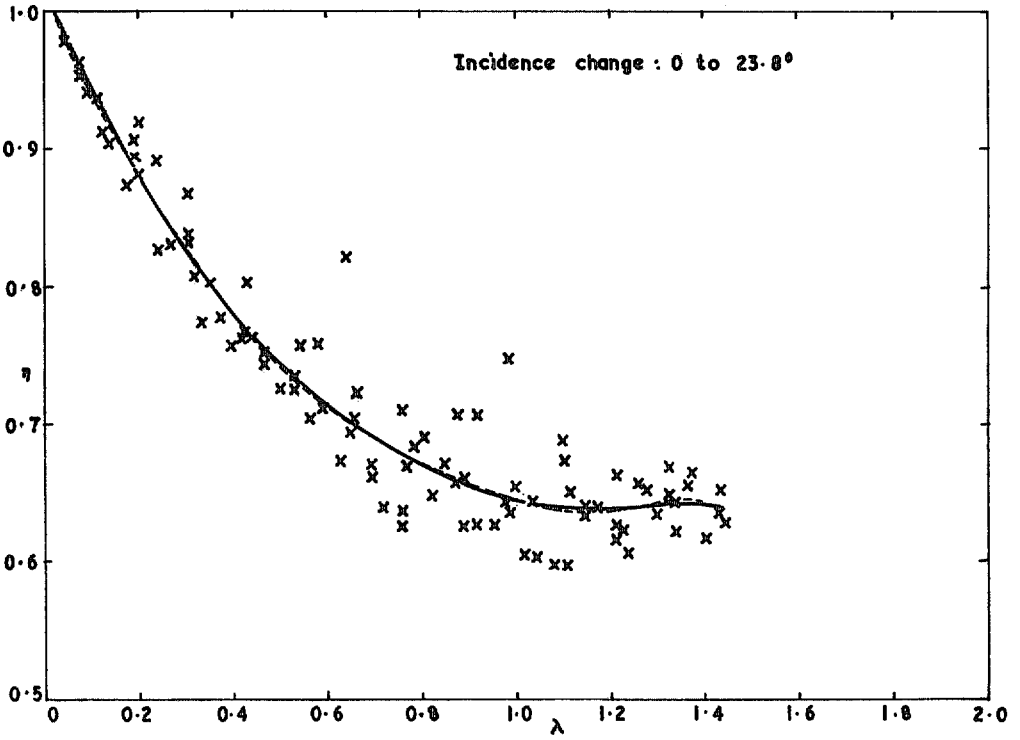

FIG. 9a. Expt. No. 4. Spanwise position of vortex centre for 40° plate $x/c_0 = 2/3$.

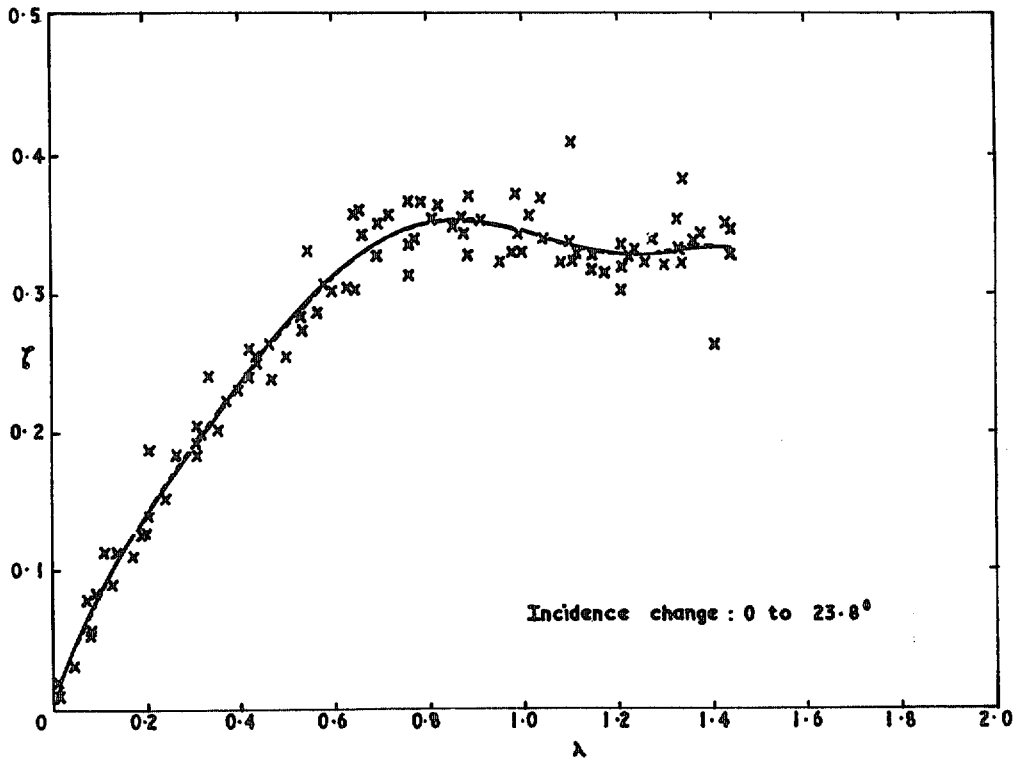

FIG. 9b. Expt. No. 4. Height of vortex centre above 40° plate $x/c_0 = 2/3$.

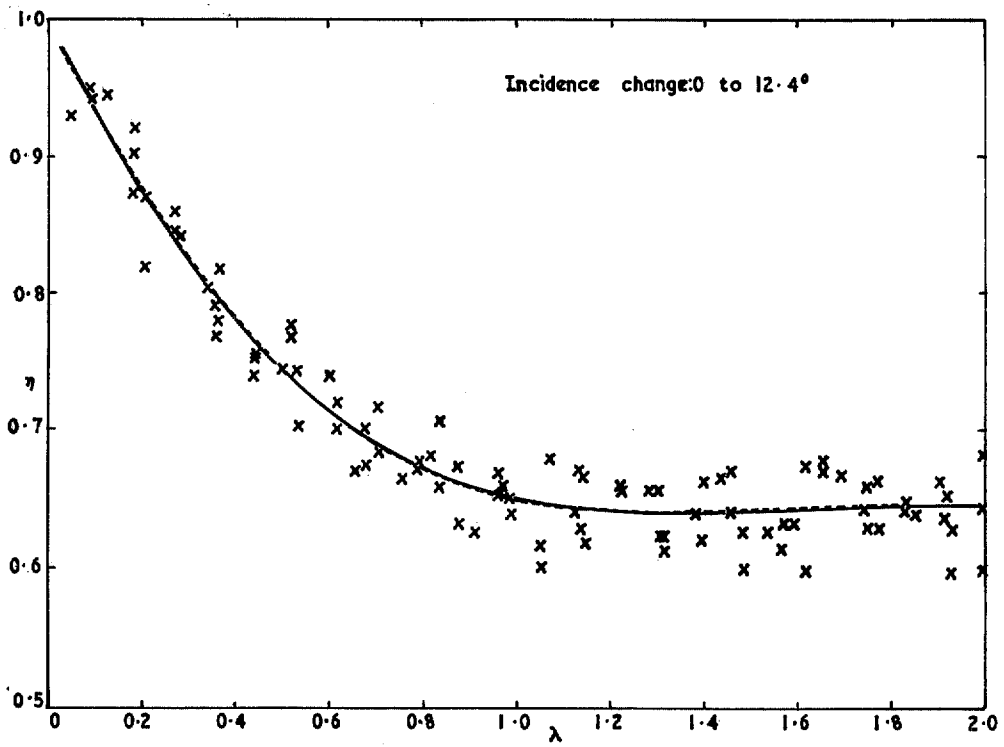

FIG. 10a. Expt. No. 5. Spanwise position of vortex centre for 40° plate $x/c_0 = 1/2$.

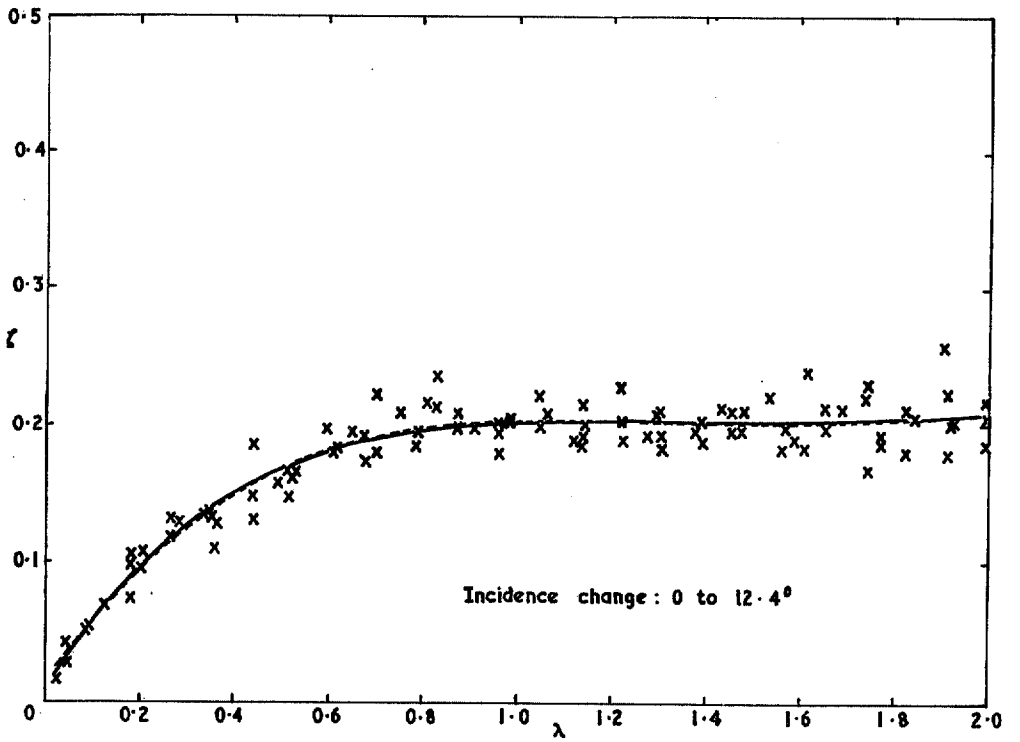

FIG. 10b. Expt. No. 5. Height of vortex centre above 40° plate $x/c_0 = 1/2$.

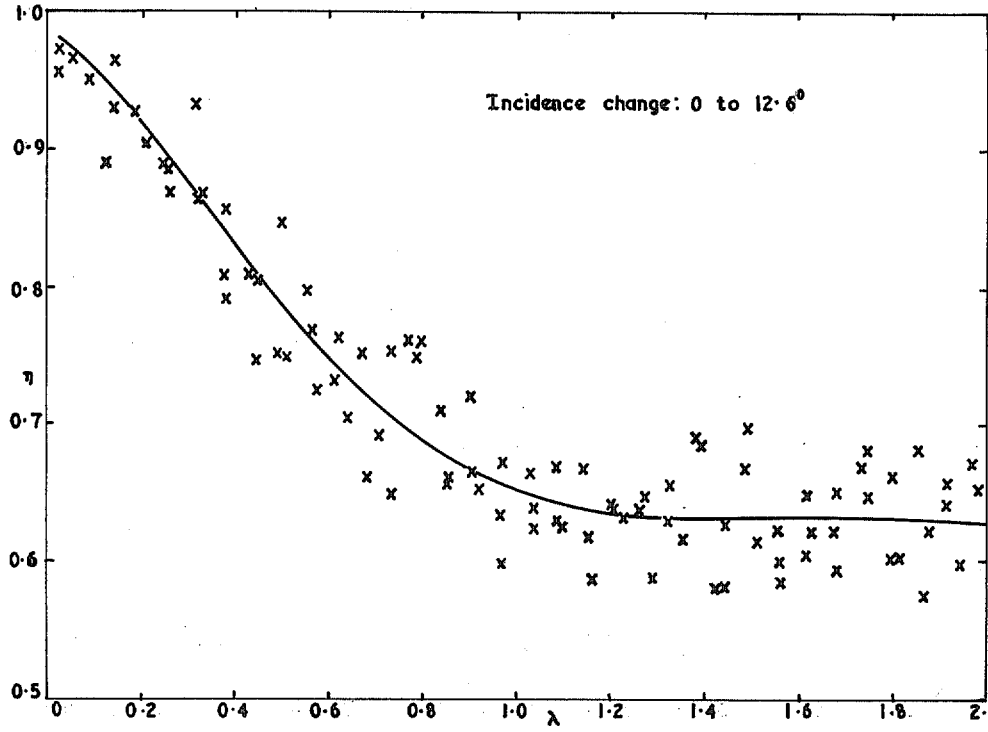

FIG. 11a. Expt. No. 6. Spanwise position of vortex centre for 40° plate $x/c_0 = 2/3$.

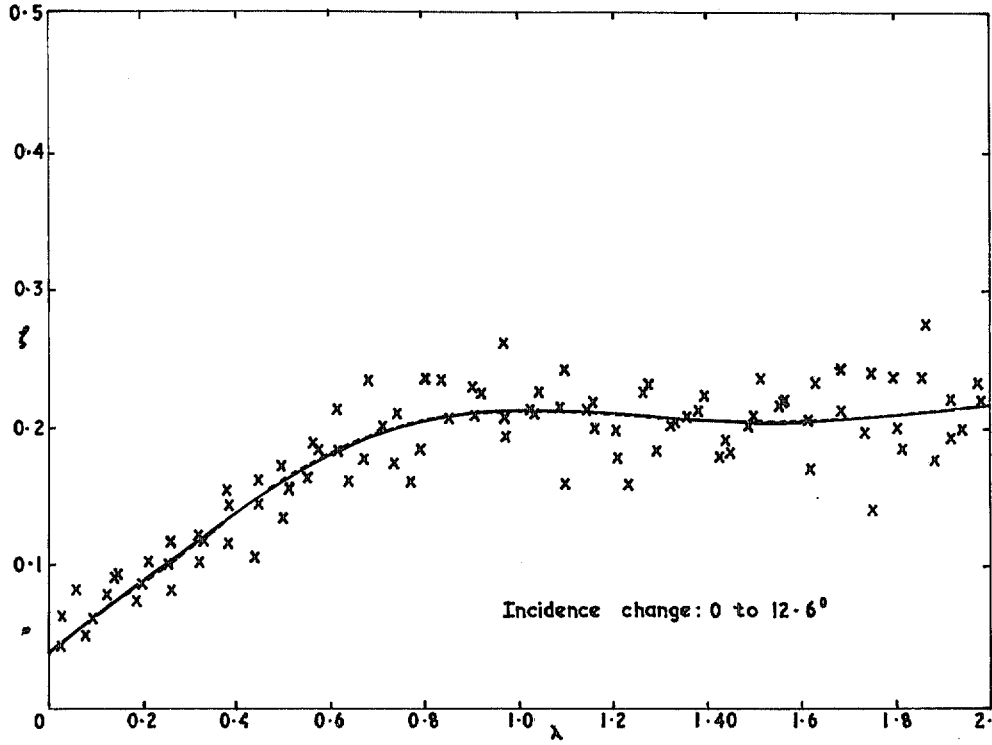

FIG. 11b. Expt. No. 6. Height of vortex centre above 40° plate $x/c_0 = 2/3$.

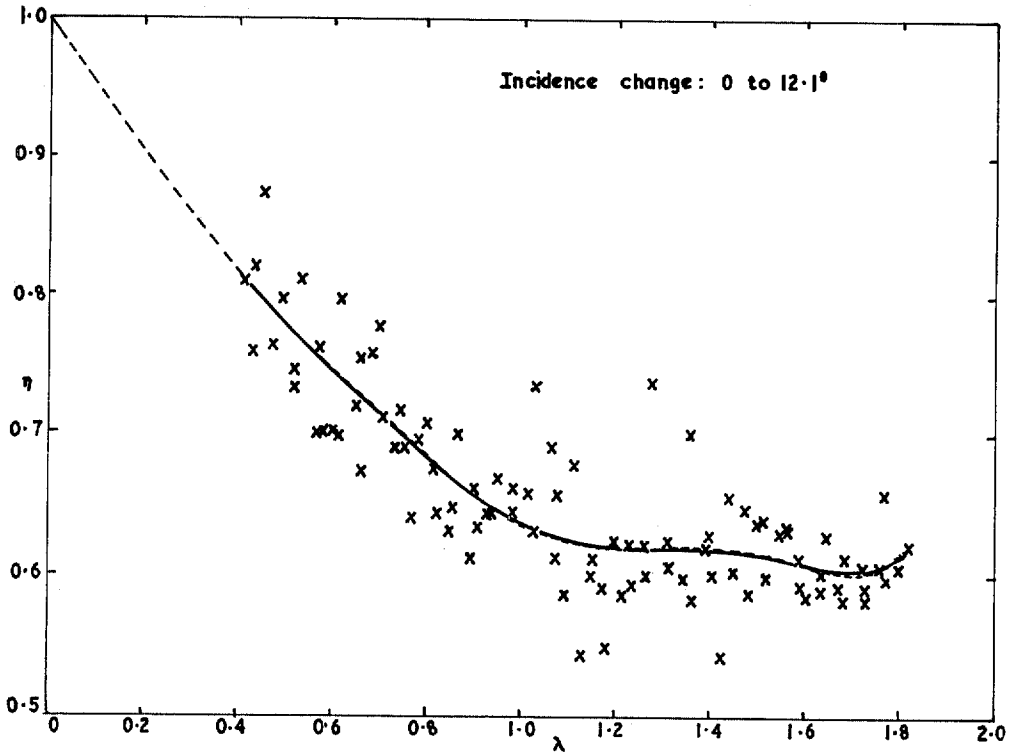

FIG. 12a. Expt. No. 7. Spanwise position of vortex centre for 40° plate $x/c_0 = 1$.

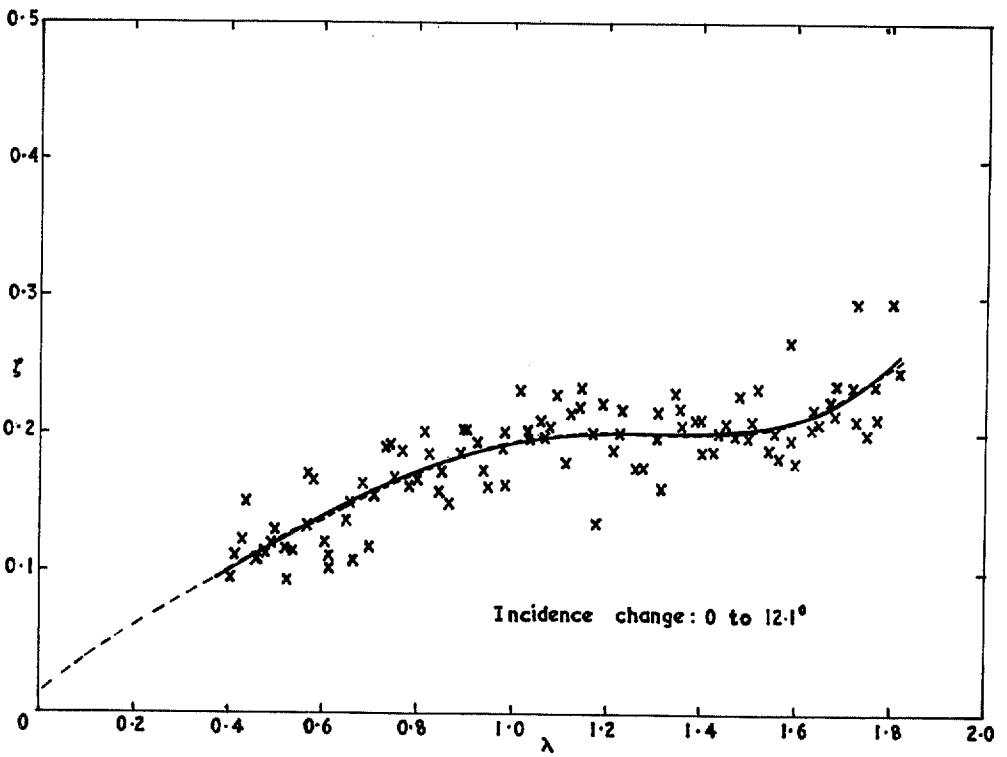

FIG. 12b. Expt. No. 7. Height of vortex centre above 40° plate $x/c_0 = 1$.

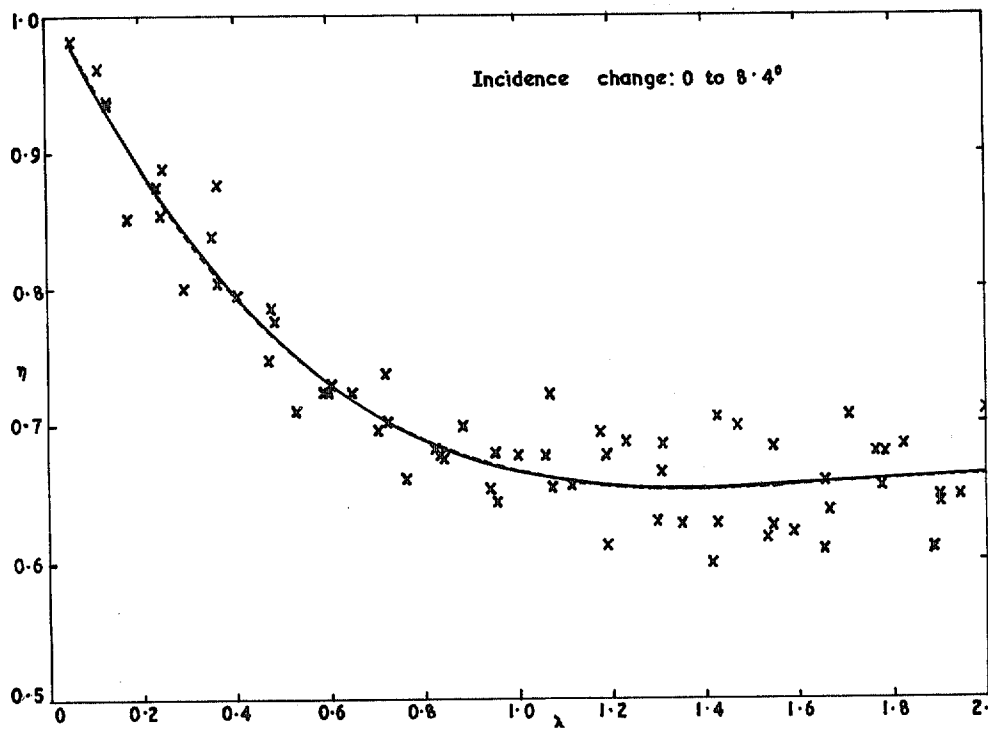

FIG. 13a. Expt. No. 8. Spanwise position of vortex centre for 40° plate $x/c_0 = 2/3$.

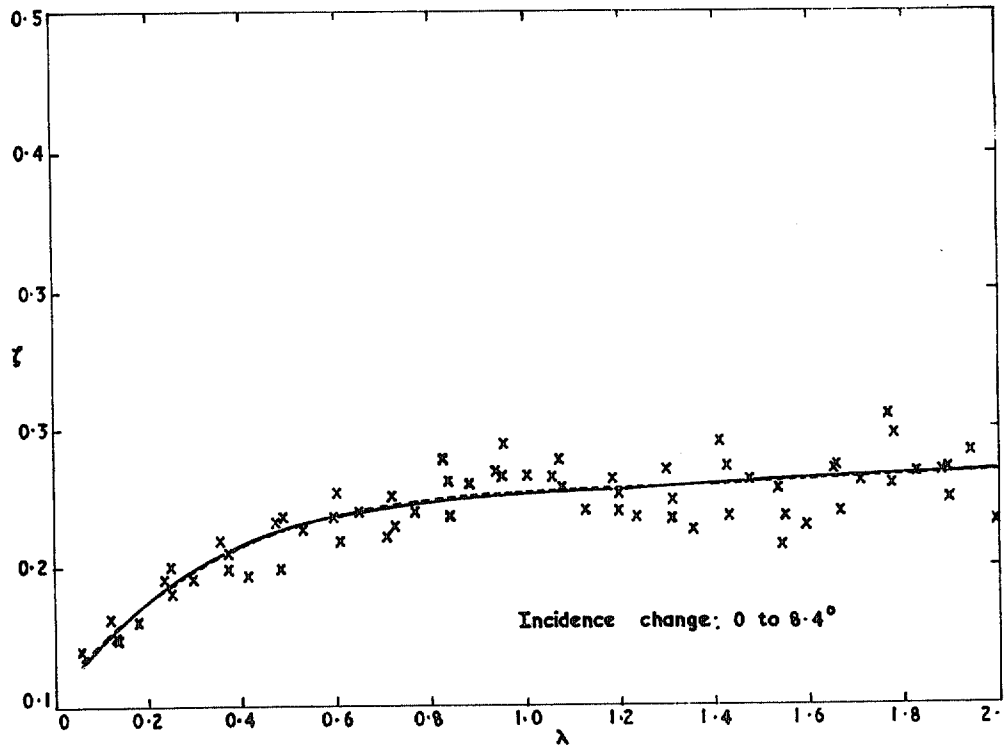

FIG. 13b. Expt. No. 8. Height of vortex centre above 40° plate $x/c_0 = 2/3$.

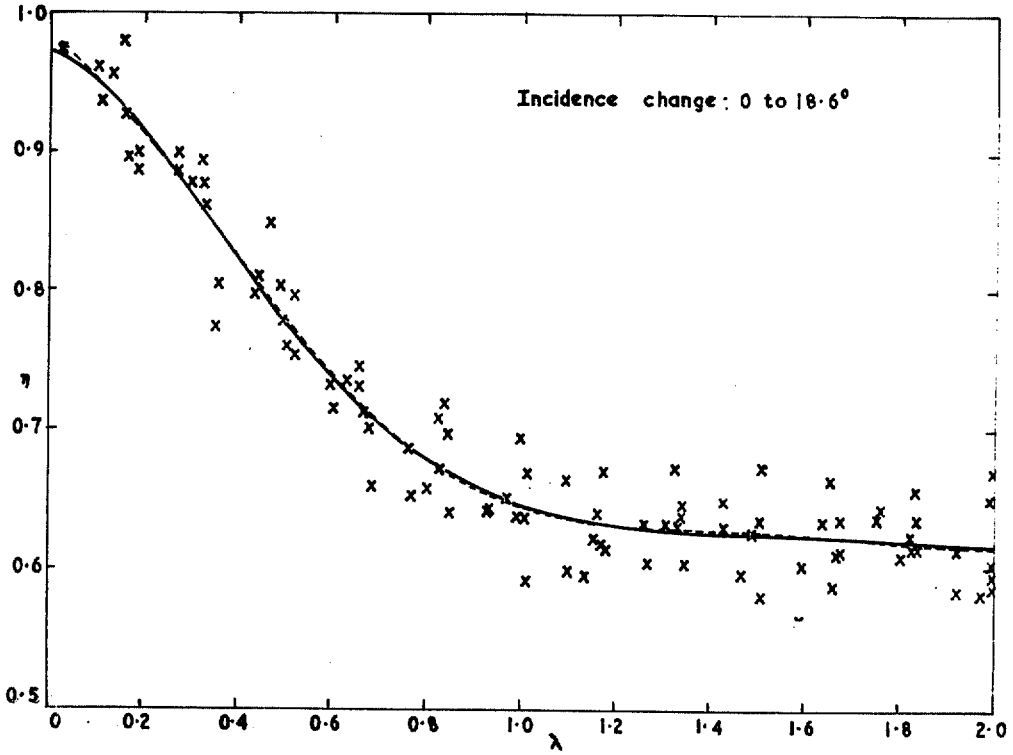

FIG. 14a. Expt. No. 9. Spanwise position of vortex centre for 60° plate $x/c_0 = 2/3$.

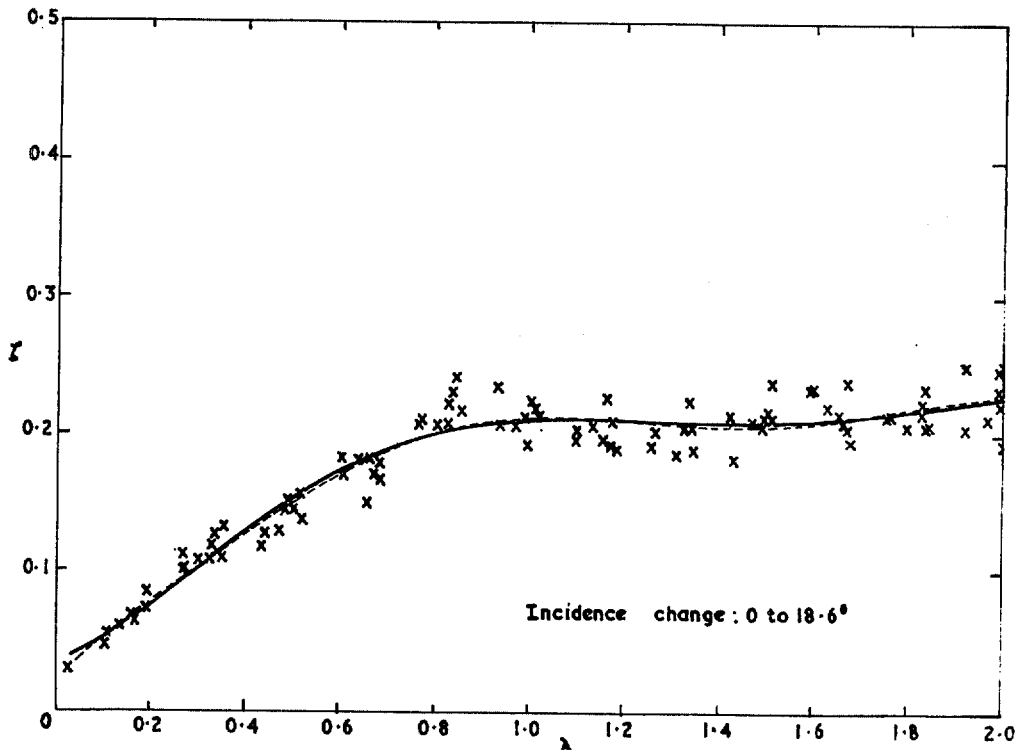

FIG. 14b. Expt. No. 9. Height of vortex centre above 60° plate $x/c_0 = 2/3$.

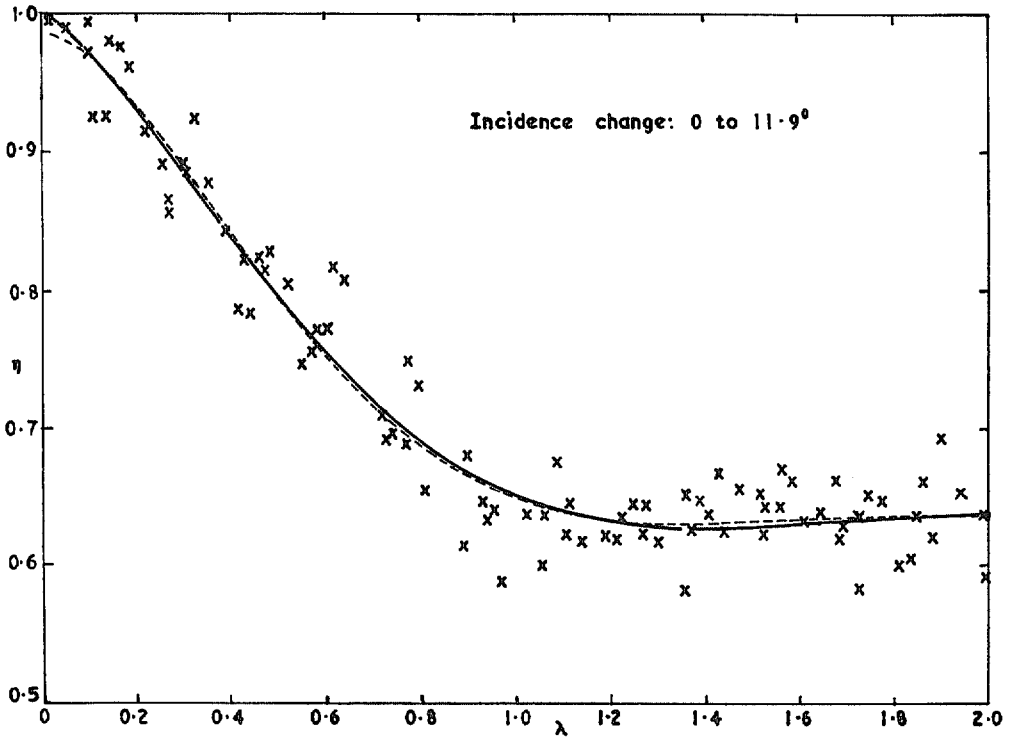

FIG. 15a. Expt. No. 10. Spanwise position of vortex centre for 60° plate $x/c_0 = 2/3$.

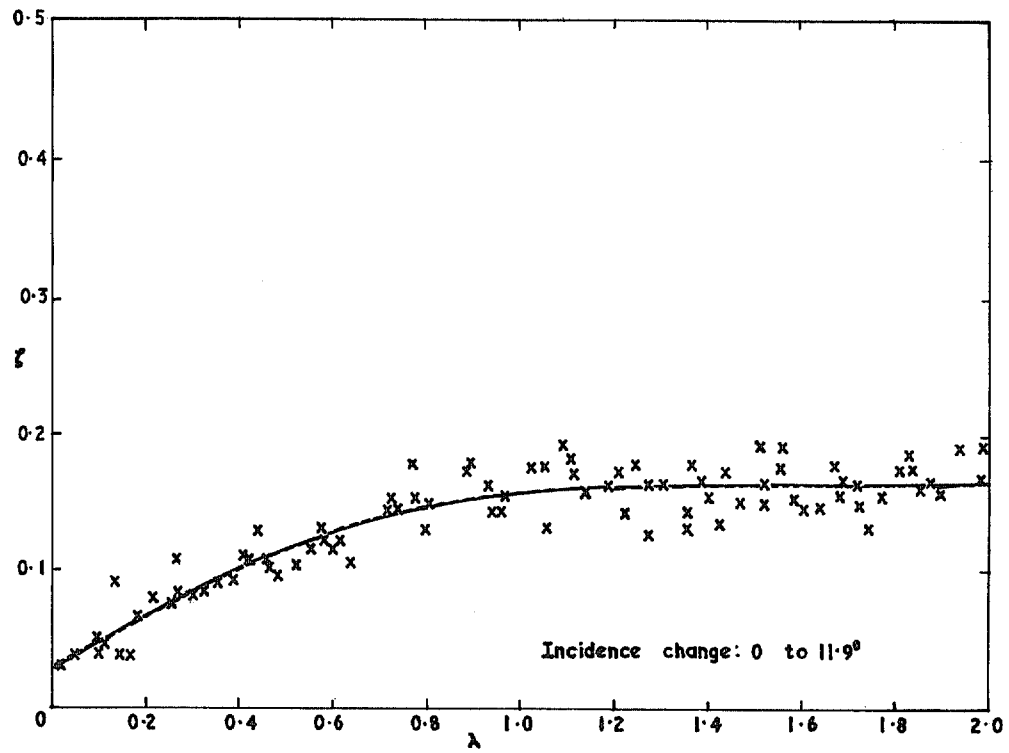

FIG. 15b. Expt. No. 10. Height of vortex centre above 60° plate $x/c_0 = 2/3$.

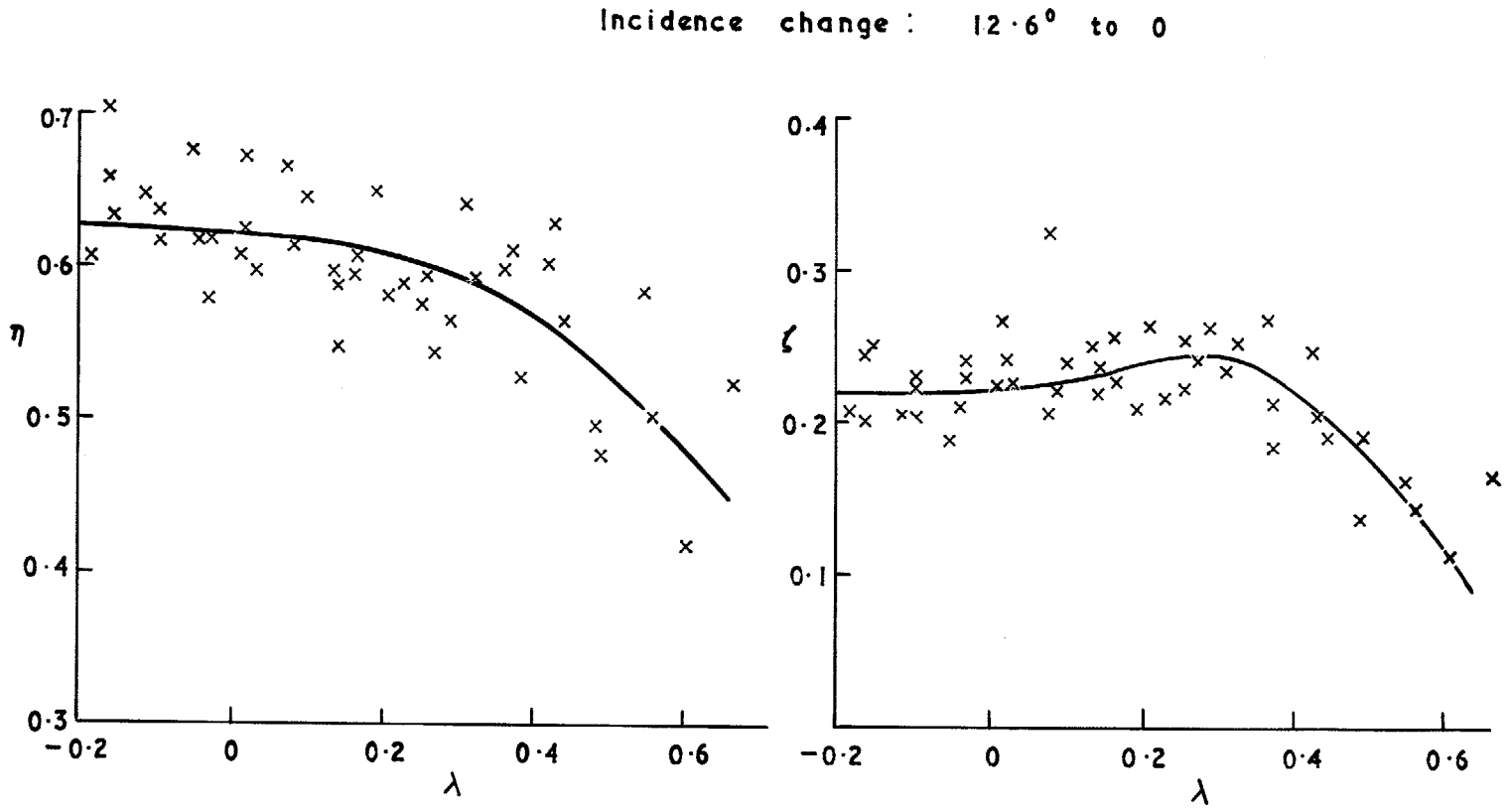

FIG. 16. Expt. No. 6. Position of vortex centre after plunge stops (40° plate) $x/c_0 = 2/3$.

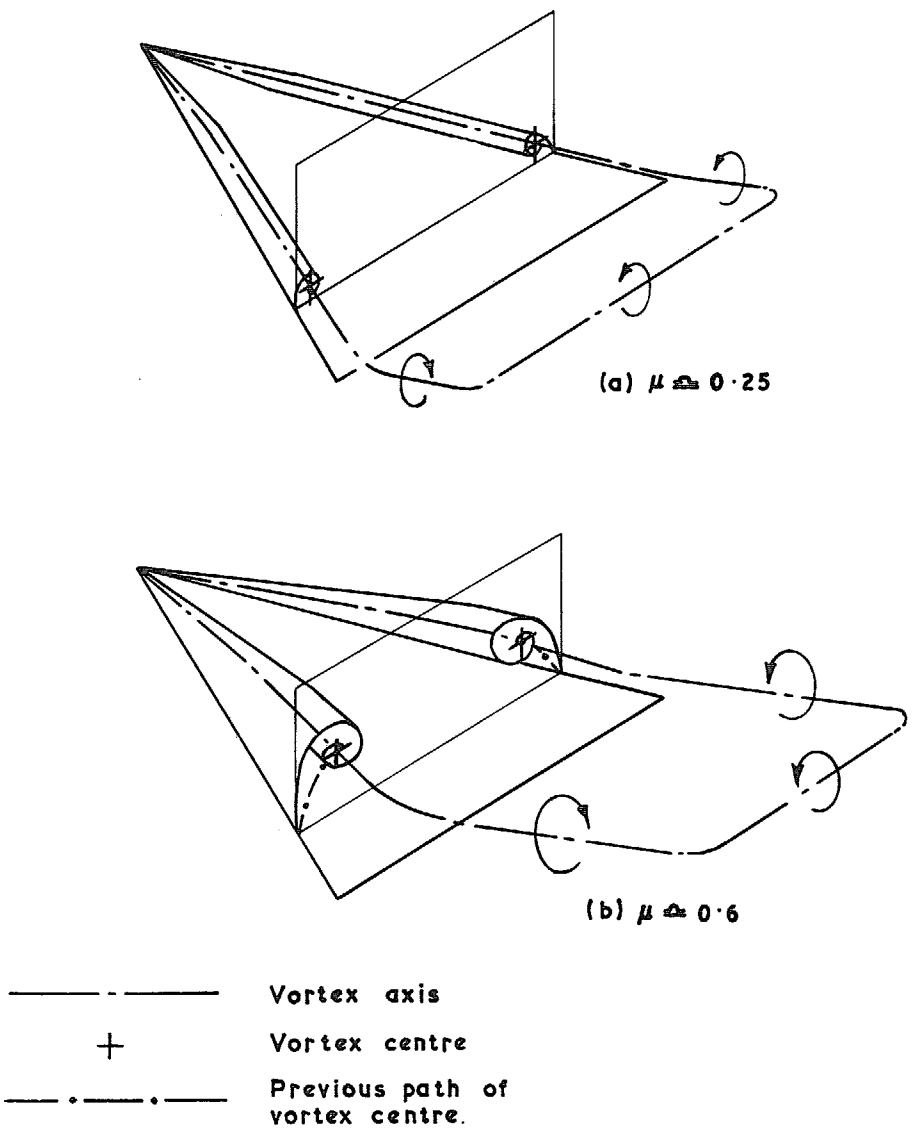

FIGS. 17a & b. Schematic representation of flow during plunge from zero to positive incidence.

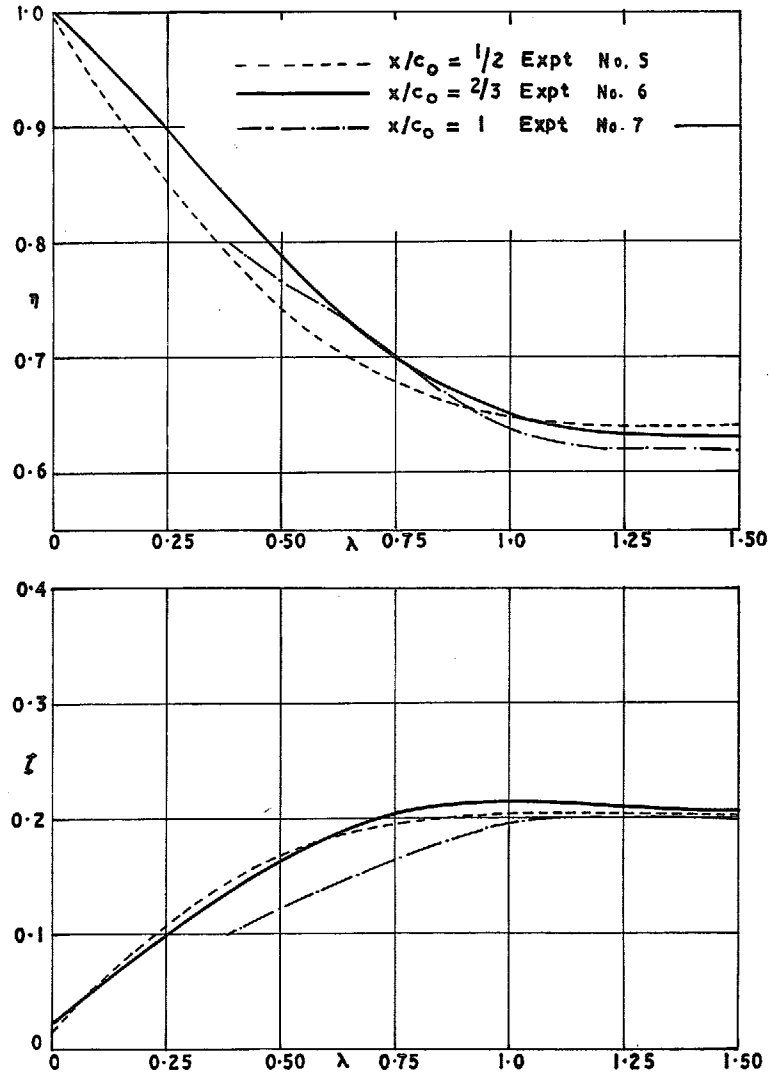

FIG. 18. Comparison of η, ζ for different chordwise position. 40° plate $\alpha_B = 12{\cdot}4°$.

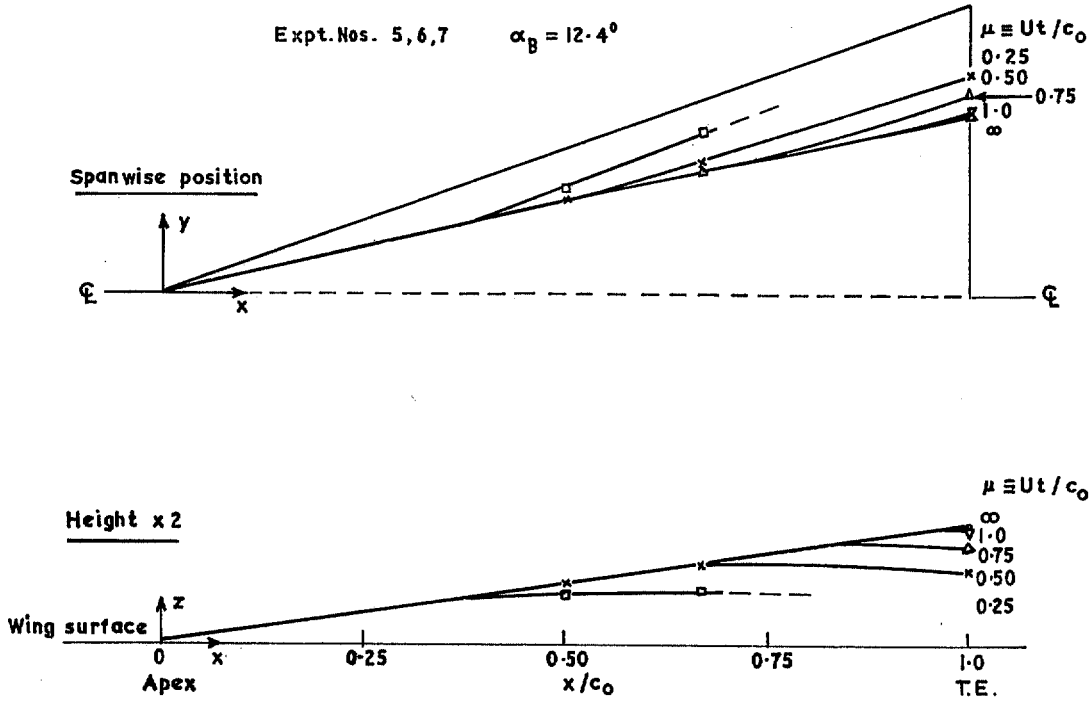

FIG. 19. Instantaneous positions of vortex axis for 40° plate.

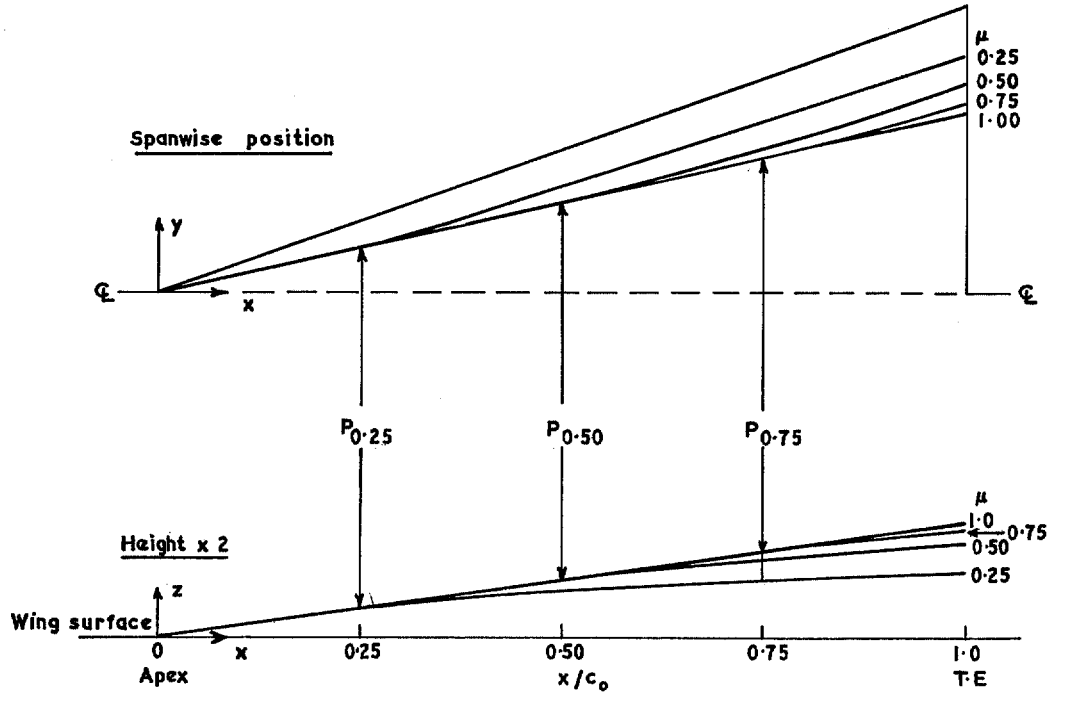

FIG. 20. Instantaneous positions of vortex axis on 40° plate. Dore's theoretical values (Ref. 4) for $\alpha_B/k = 0{\cdot}54$ adjusted to give agreement with experiment for $\mu \to \infty$ (Points $P\mu$ denote demarcation upstream of which vortex has achieved its final position).

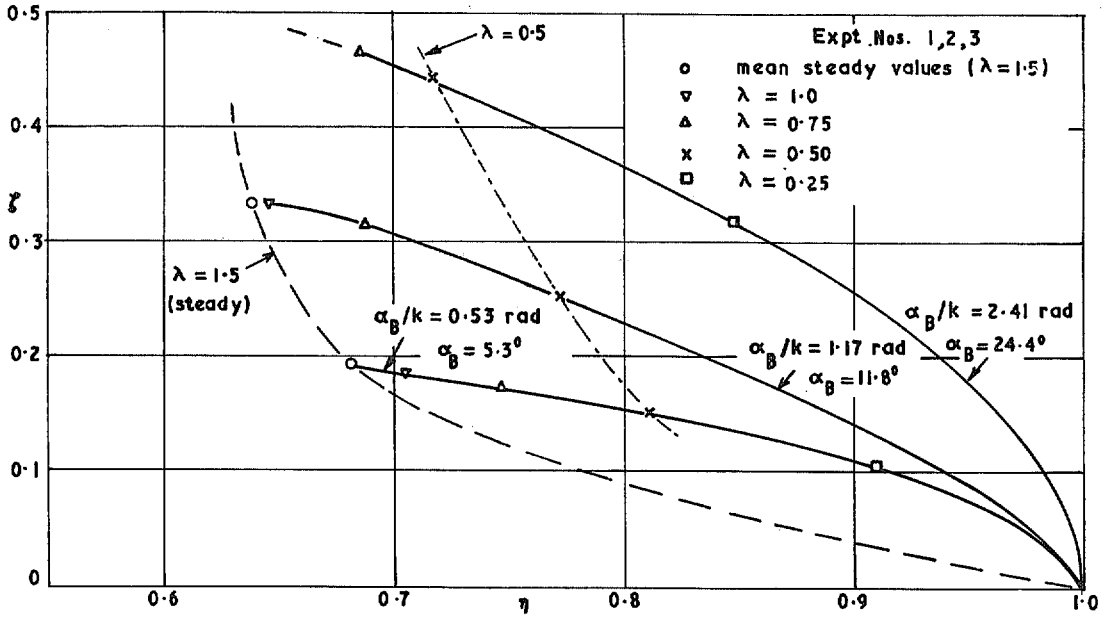

FIG. 21. Vortex paths in a cross-flow plane for 20° plate $x/c_0 = 2/3$.

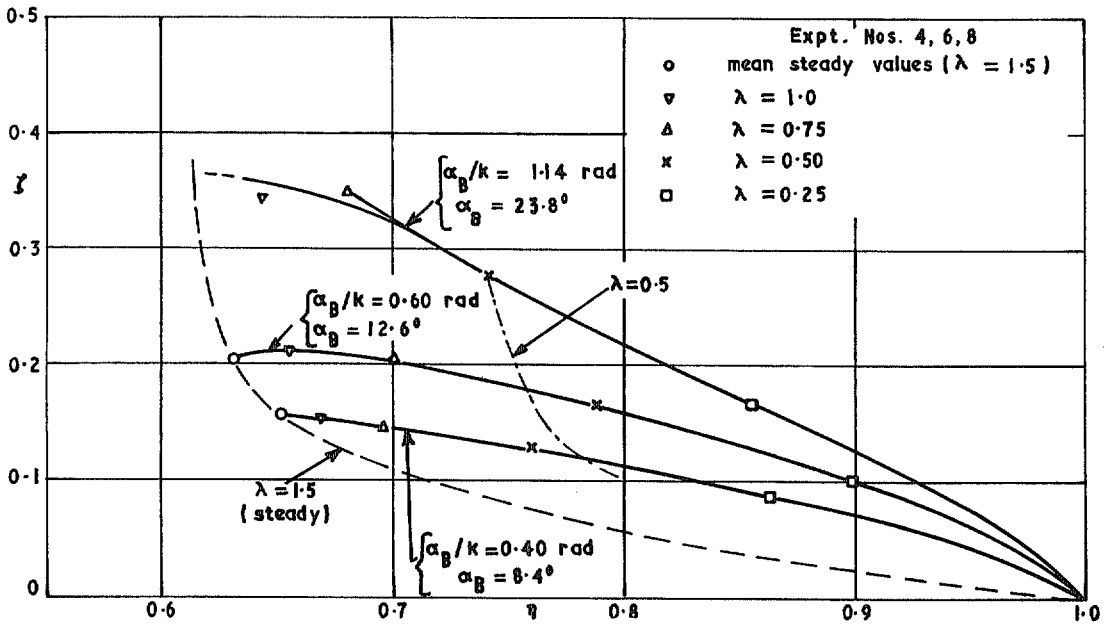

FIG. 22. Vortex paths in a cross-flow plane for 40° plate $x/c_0 = 2/3$.

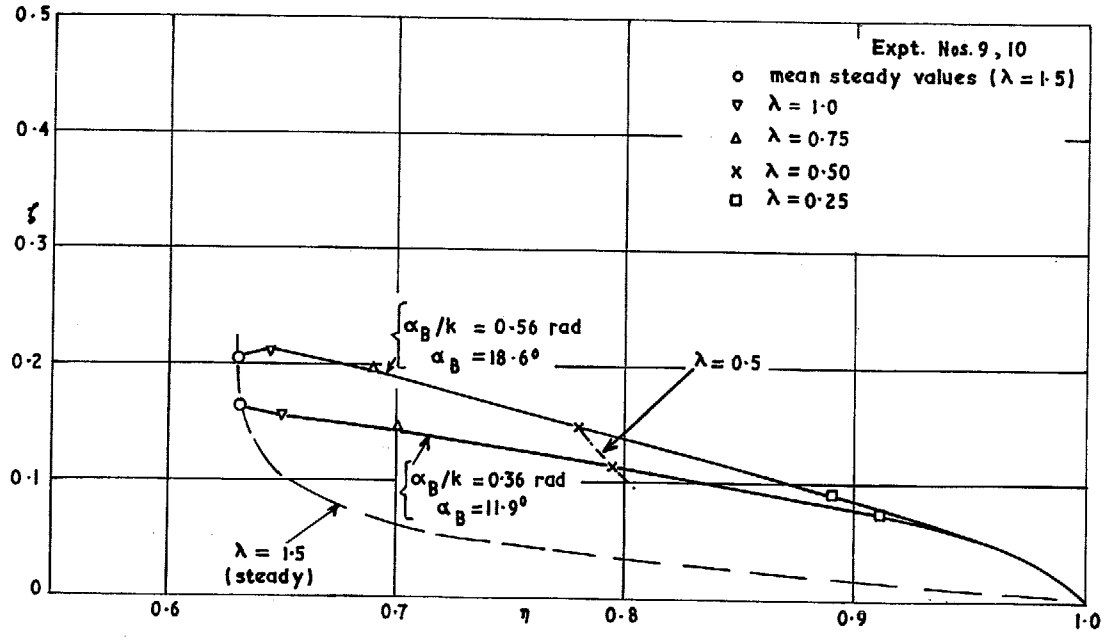

FIG. 23. Vortex paths in a cross-flow plane for 60° plate $x/c_0 = 2/3$.

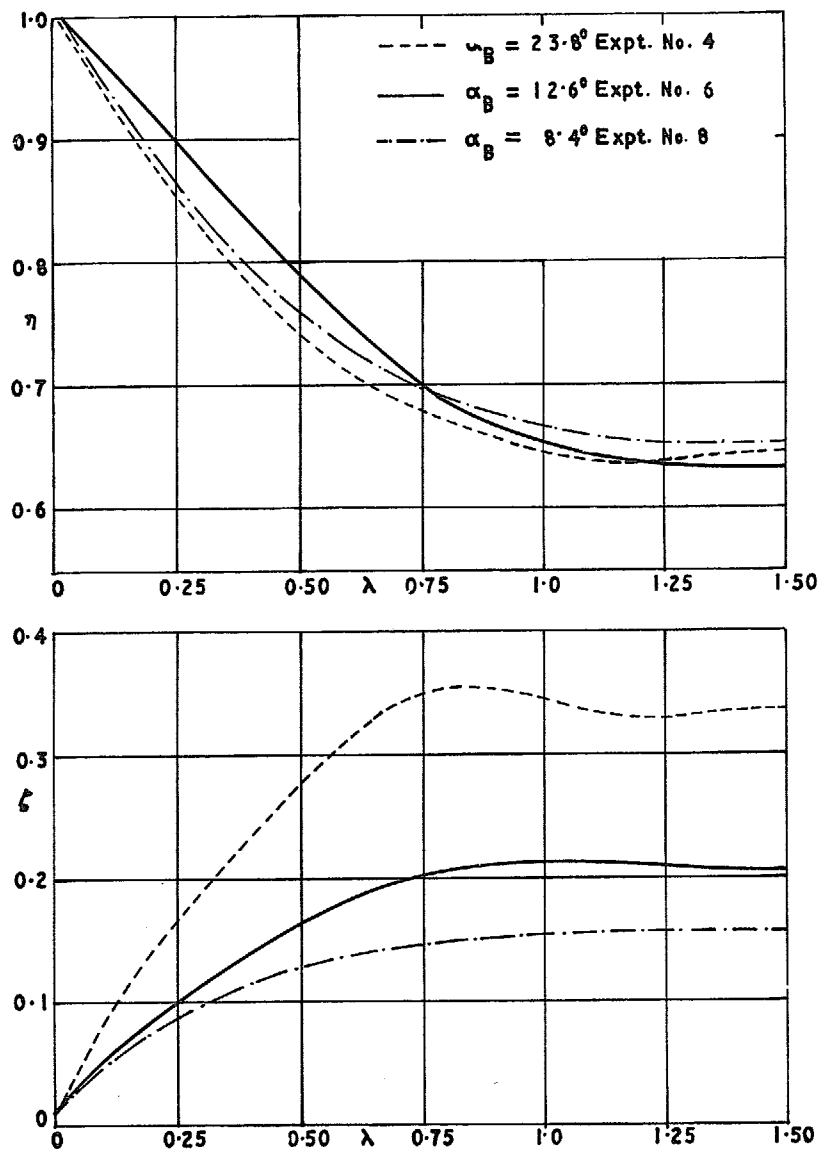

FIG. 24. Comparison of η, ζ for different values α_B, 40° plate.

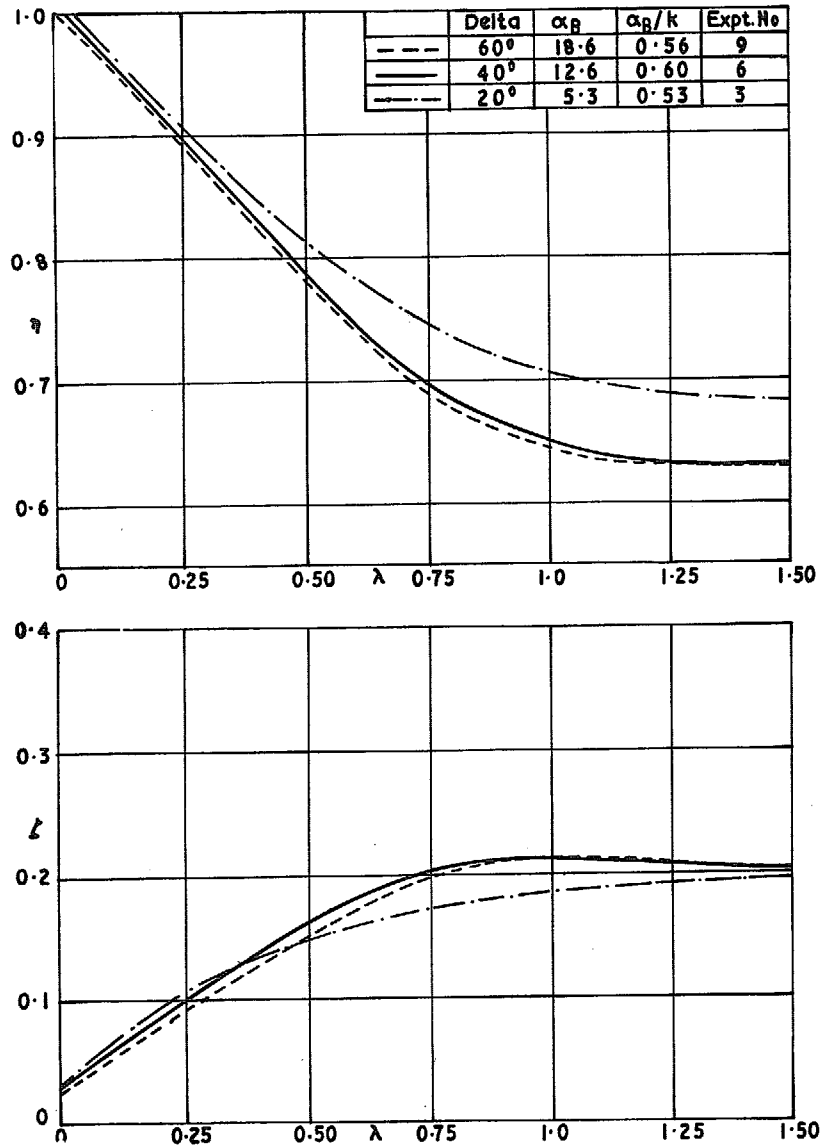

FIG. 25. Comparison of η, ζ for different plates at approximately the same values of α_B/k.

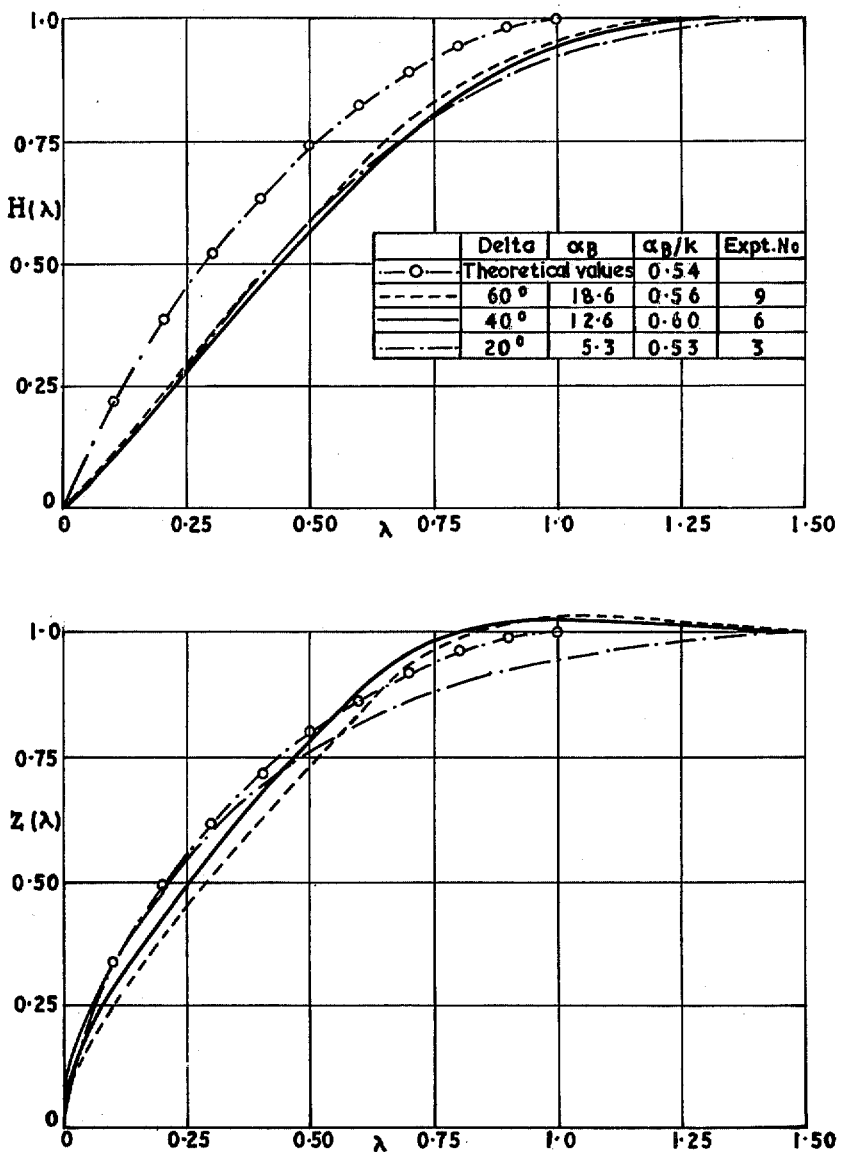

FIG. 26. Comparison of $H(\lambda)$, $Z(\lambda)$ for different plates at approximately the same value of α_B/k.

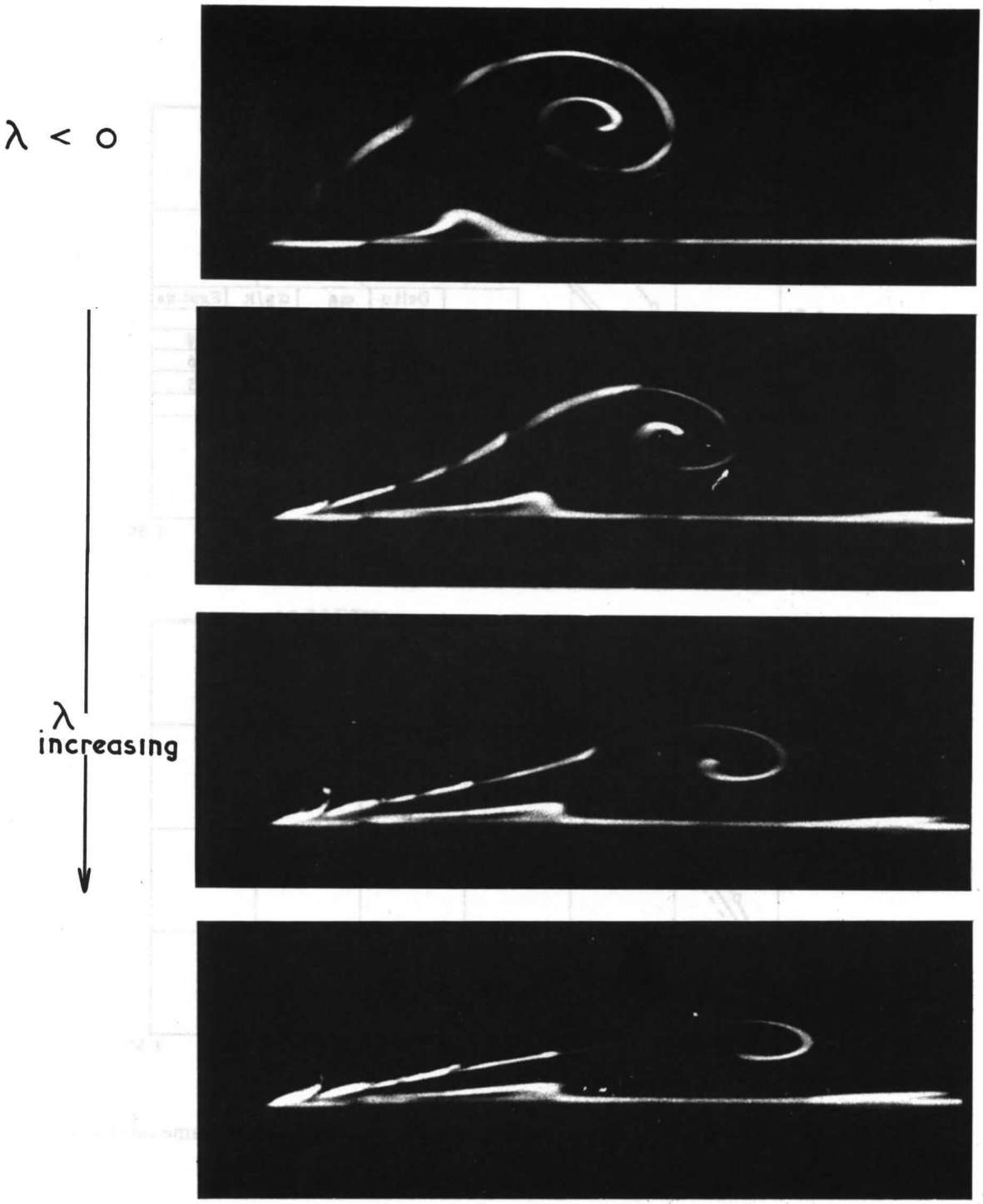

FIG. 27. Changes in the shape of the vortex layer following a decrease from positive to zero incidence. (Photographs show approx. half local span).

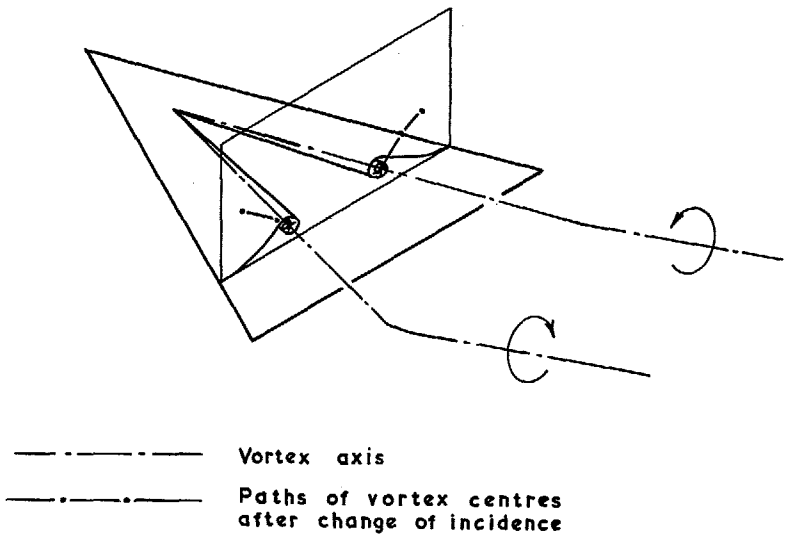

FIG. 28. Convection of vortex system after change from positive to zero incidence.

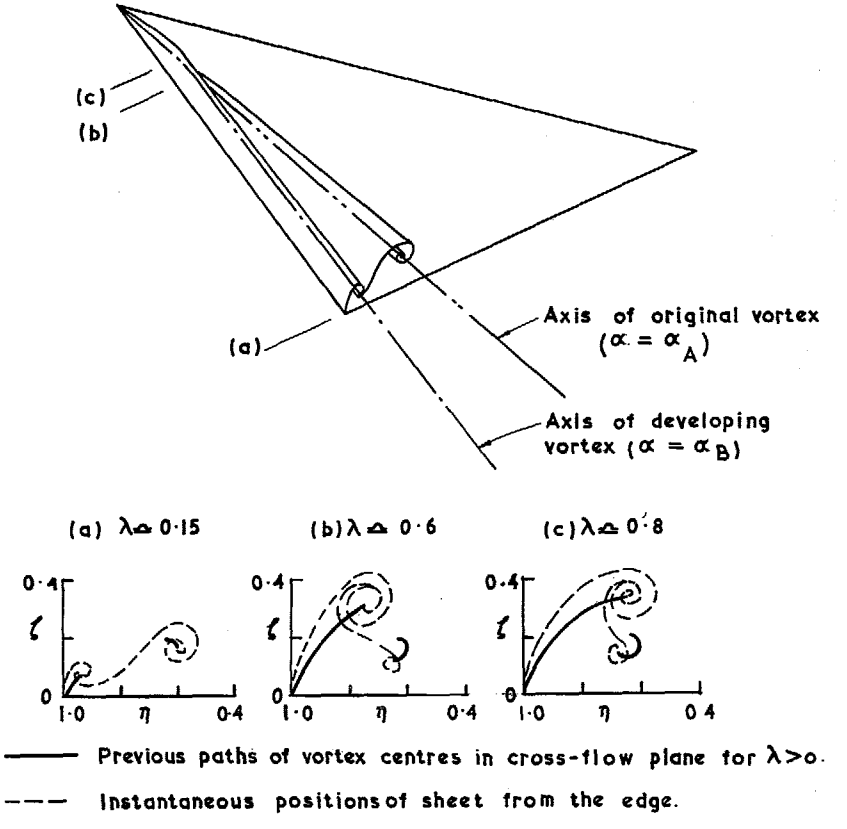

FIG. 29. Transitional vortex flow following a change from positive incidence ($\alpha_A \simeq 11°$) to higher positive incidence ($\alpha_B \simeq 22°$).

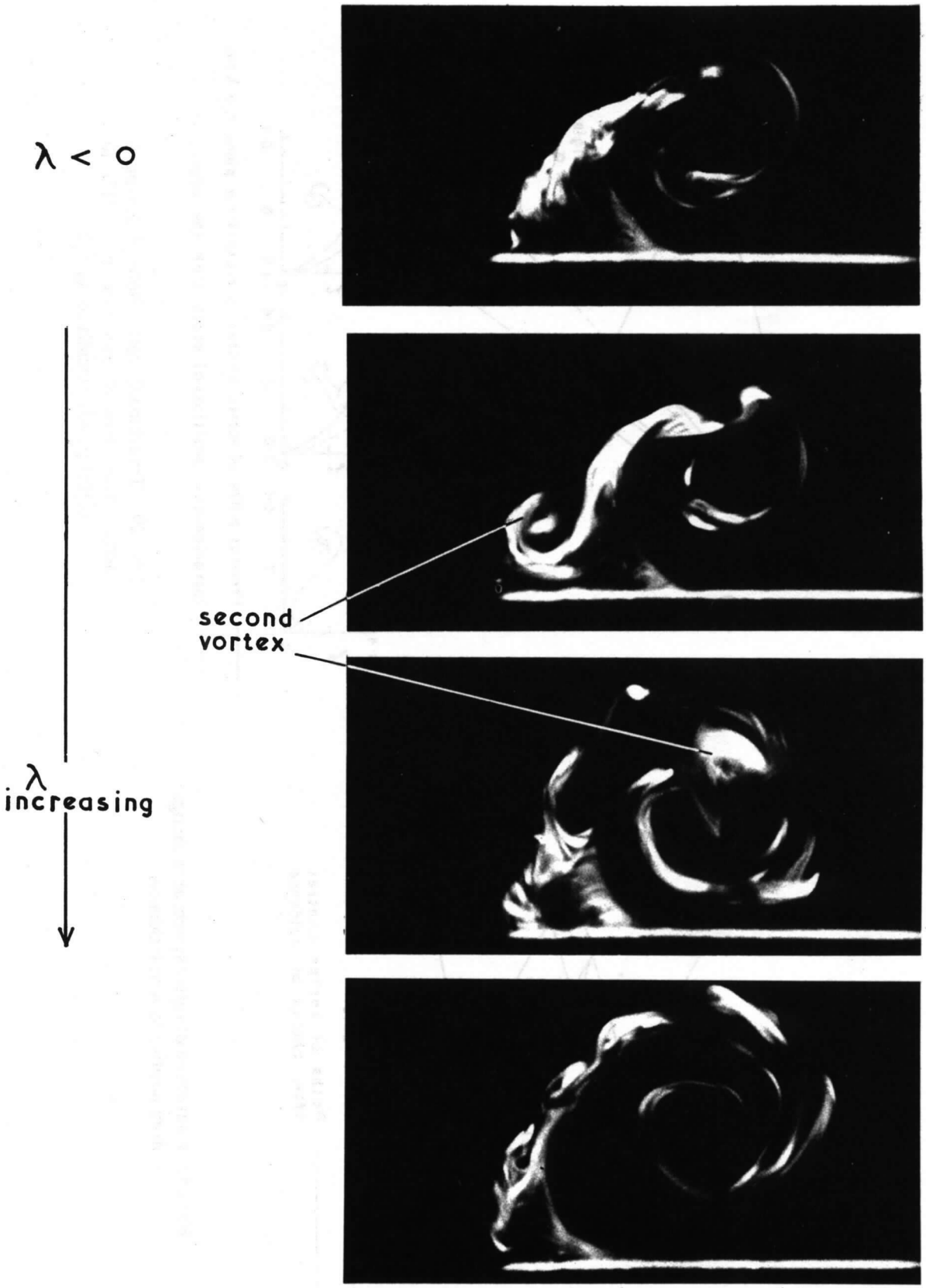

FIG. 30. Changes in the vortex layer following an increase from 11° to 18° incidence.

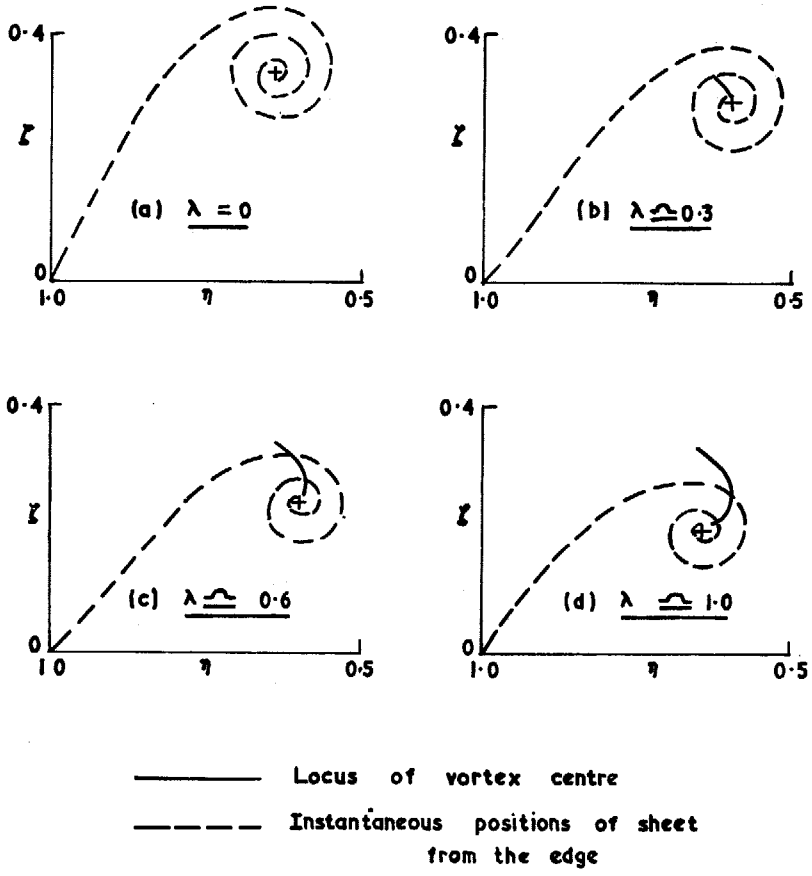

FIG. 31. Development of vortex flow in cross-flow plane after change from positive incidence ($\alpha_A \simeq 22°$) to lower positive incidence ($\alpha_B \simeq 11°$).

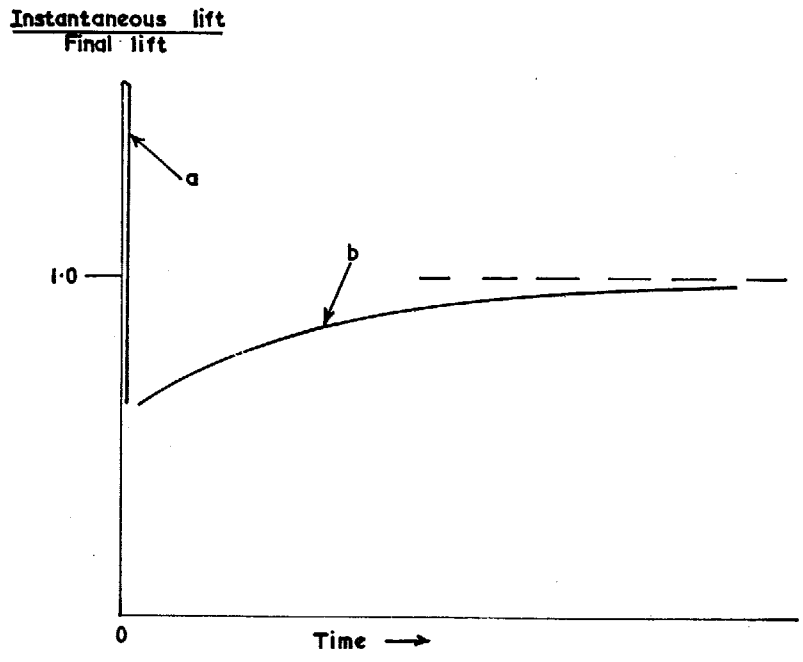

FIG. 32. General form of transient lift following sudden change of incidence.

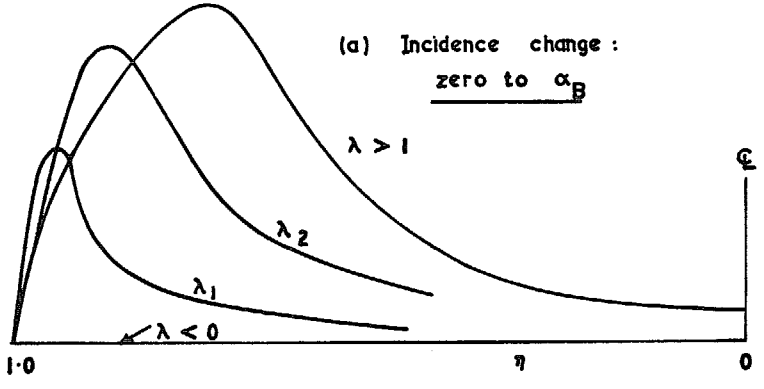

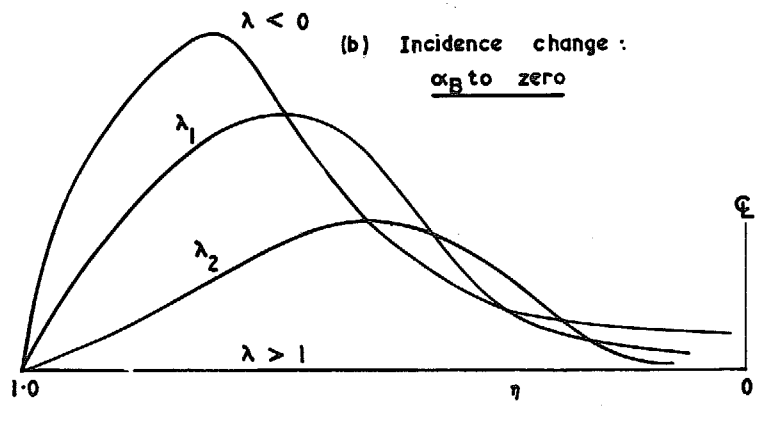

FIGS 33 a & b. Suggested forms of transient spanwise lift distribution ($\alpha_A = 0; \alpha_B > 0$).

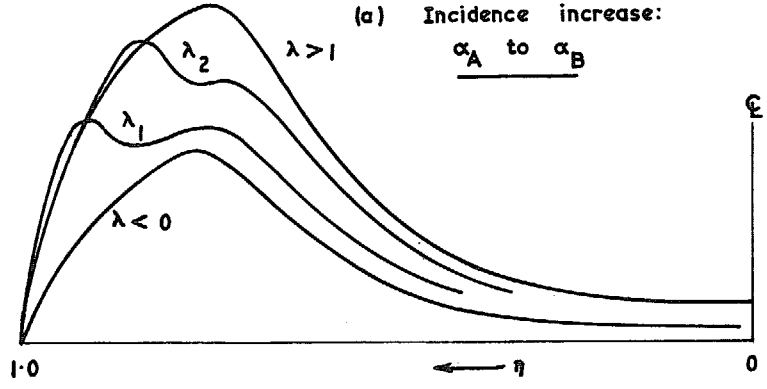

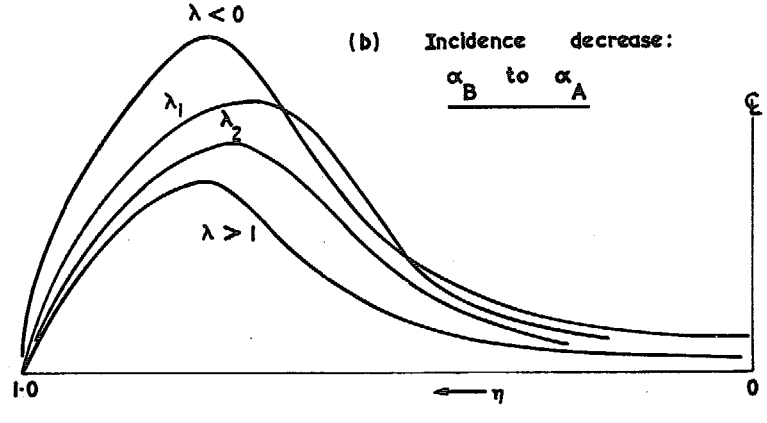

FIG. 34 a & b. Suggested forms of transient spanwise lift distribution ($0 < \alpha_A < \alpha_B$).

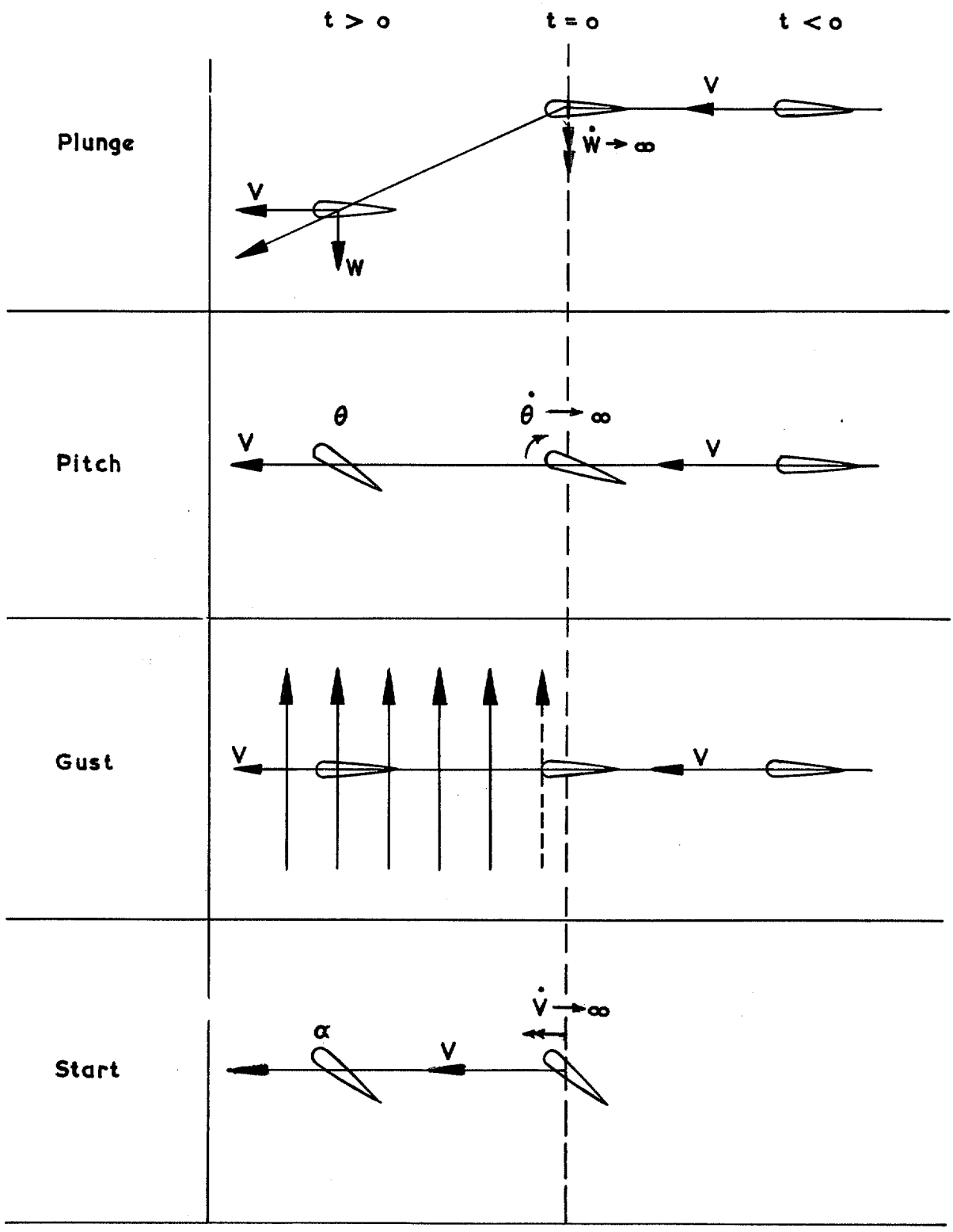

FIG. 35. Types of change resulting in growth of lift.

Printed in Wales for Her Majesty's Stationery Office by Allens Printers (Wales) Limited

Dd. 501372 K.5

Published by
HER MAJESTY'S STATIONERY OFFICE

To be purchased from
49 High Holborn, London WC1V 6HB
13a Castle Street, Edinburgh EH2 3AR
109 St Mary Street, Cardiff CF1 1JW
Brazennose Street, Manchester M60 8AS
50 Fairfax Street, Bristol BS1 3DE
258 Broad Street, Birmingham B1 2HE
7 Linenhall Street, Belfast BT2 8AY
or through booksellers

SBN 11 470365 5